1 **Biogenic and anthropogenic sources of isoprene and monoterpenes and their secondary organic**
2 **aerosol in Delhi, India**

3 Daniel J. Bryant[1], Beth S. Nelson[1], Stefan J. Swift[1a], Sri Hapsari Budisulistiorini[1], Will S. Drysdale[1,2],
4 Adam R. Vaughan[1], Mike J. Newland[1b], James R. Hopkins[1,2], James M. Cash[3,4], Ben Langford[3], Eiko
5 Nemitz[3], W. Joe F. Acton[5c], C. Nicholas Hewitt[5], Tuhin Mandal[6], Bhola R. Gurjar[6], Shivani[6d], Ranu
6 Gadi[6], James D. Lee[1,2], Andrew R. Rickard[1,2], Jacqueline F. Hamilton[1]

7 1- Wolfson Atmospheric Chemistry Laboratories, Department of Chemistry, University of York,
8 Heslington, York, YO10 5DD, UK

9 2- National Centre for Atmospheric Science, University of York, Heslington, York, YO10 5DD, UK

10 3- UK Centre for Ecology and Hydrology, Penicuik, Midlothian, Edinburgh, EH26 0QB, UK

11 4- School of Chemistry, University of Edinburgh, Edinburgh, EH9 3FJ, Edinburgh, UK

12 5- Lancaster Environment Centre, Lancaster University, Lancaster, LA1 4YW, UK

13 6- Department of Applied Sciences and Humanities, Indira Gandhi Delhi Technical University for
14 Women, Delhi, 110006, India

15 [a] now at: J. Heyrovsky Institute of Physical Chemistry, Department of Chemistry of Ions in Gaseous
16 Phase, Prague, Czech Republic

17 [b] now at: ICARE-CNRS, 1 C Av. de la Recherche Scientifique, 45071 Orléans CEDEX 2, France

18 [c] now at: School of Geography, Earth and Environmental Sciences, University of Birmingham,
19 Birmingham, B15 2TT, UK

20 [d] now at: Department of Chemistry, Miranda House, Delhi University, Delhi, 110007, India

21 Correspondence email: daniel.bryant@york.ac.uk

22 **Abstract**

23 Isoprene and monoterpenes emissions to the atmosphere are generally dominated by biogenic
24 sources. The oxidation of these compounds can lead to the production of secondary organic aerosol,
25 however the impact of this chemistry in polluted urban settings has been poorly studied. Isoprene
26 and monoterpenes can form SOA heterogeneously via anthropogenic-biogenic interactions resulting
27 in the formation of organosulfates (OS) and nitrooxy-organosulfates (NOS). Delhi, India is one of the
28 most polluted cities in the world, but little is known about the emissions of biogenic VOCs or the
29 sources of SOA. As part of the DELHI-FLUX project, gas phase mixing ratios of isoprene and speciated
30 monoterpenes were measured during pre- and post-monsoon measurement campaigns in central
31 Delhi. Nocturnal mixing ratios of the VOCs were substantially higher during the post-monsoon
32 (isoprene: (0.65 ± 0.43) ppbv, limonene: (0.59 ± 0.11) ppbv, α-pinene: (0.13 ± 0.12) ppbv) than the
33 pre-monsoon (isoprene: (0.13 ± 0.18) ppbv, limonene: 0.011 ± 0.025 (ppbv), α-pinene: $0.033 \pm$
34 0.009) period. At night, isoprene and monoterpene concentrations correlated strongly with CO
35 across during the post-monsoon period. Filter samples of particulate matter less than 2.5 microns in
36 diameter ($PM_{2.5}$) were collected and the OS and NOS content analysed using ultrahigh-performance
37 liquid chromatography tandem mass spectrometry (UHPLC-MS[2]). Inorganic sulfate was shown to
38 facilitate the formation of isoprene OS species across both campaigns. Sulfate contained within OS
39 and NOS species were shown to contribute significantly to the sulfate signal measured via AMS.
40 Strong nocturnal enhancements of NOS species were observed across both campaigns. The total

concentration of OS/NOS species contributed an average of (2.0 ± 0.9) % and (1.8 ± 1.4) % to the total oxidised organic aerosol, and up to a maximum of 4.2 % and 6.6 % across the pre- and post-monsoon periods, respectively. Overall, this study provides the first molecular level measurements of SOA derived from isoprene and monoterpene in Delhi and demonstrates that both biogenic and anthropogenic sources of these compounds can be important in urban areas.

1. Introduction

India is undergoing significant urbanization and industrialisation, with a rapidly increasing population. According to the WHO, India was home to 9 out of the top 10 most polluted cities in the world in 2020 in terms of annual mean $PM_{2.5}$ (particulate matter less than 2.5 micrometres in diameter) concentrations (WHO, 2018). In Delhi, the population-weighted mean $PM_{2.5}$ was estimated to be 209 (range: 120 – 339.5) $\mu g\ m^{-3}$ in 2017, over 40 times the WHO annual mean guidelines of 5 $\mu g\ m^{-3}$, and greater than five times India's own standard of 40 $\mu g\ m^{-3}$ (Balakrishnan et al., 2019). Air pollution is estimated to cause over 1 million deaths per year in India alone (Landrigan et al., 2018).

Numerous studies have investigated $PM_{2.5}$ concentrations, characteristics and meteorological effects in Delhi (Anand et al., 2019; Bhandari et al., 2020; Chowdhury et al., 2004; Hama et al., 2020; Kanawade et al., 2020; Miyazaki et al., 2009; Nagar et al., 2017). The key sources of $PM_{2.5}$ identified are secondary aerosol, fossil fuel combustion, municipal waste and biomass burning (Chowdhury et al., 2004; Sharma and Mandal, 2017; Stewart et al., 2021b, 2021a). Previous studies have also shown that alongside extremely high emissions of pollutants, regional sources and meteorology in particular play an important role in high pollution events in Delhi (Bhandari et al., 2020; Sawlani et al., 2019; Schnell et al., 2018; Sinha et al., 2014).

Secondary species have been shown to be significant contributors to PM_1 and $PM_{2.5}$ mass in Delhi, with organics contributing 40-70 % of PM_1 mass. (Gani et al., 2019; Shivani et al., 2019; Reyes-Villegas et al., 2021; Sharma and Mandal, 2017) However, limited molecular level analysis of organic aerosol (OA) has been undertaken (Chowdhury et al., 2004; Elzein et al., 2020; Miyazaki et al., 2009; Singh et al., 2021, 2012; Yadav et al., 2021). Kirillova et al., (2014) analysed the sources of water-soluble organic carbon (WSOC) in Delhi, using radiocarbon measurement constraints. The study identified that 79 % of WSOC was classified as non-fossil carbon, attributed to biogenic/biomass burning sources in urban Delhi (Kirillova et al., 2014), similar to other studies from India (Kirillova et al., 2013; Sheesley et al., 2012). Studies across Asia, Europe and North America have also shown high contributions from non-fossil sources to ambient PM concentrations in urban environments (Du et al., 2014; Kirillova et al., 2010; Szidat et al., 2004; Wozniak et al., 2012). The sources of this modern carbon in urban areas are poorly understood, although biomass burning is a key component (Elser et al., 2016; Hu et al., 2016; Lanz et al., 2010; Nagar et al., 2017). Recently in Delhi, solid-fuel combustion sources such as cow dung cake or municipal solid waste have been shown to release over 1000 different organic components into the aerosol phase at emission (Stewart et al., 2021a). Alongside biomass burning, one potential source of this non-fossil aerosol is biogenic secondary organic aerosol (BSOA), which is formed via the oxidation of biogenic volatile organic compounds (BVOCs) and subsequent gas-particle phase transfer (Hallquist et al., 2009; Hoffmann et al., 1997).

Isoprene is the most abundant BVOC, with annual global emissions estimates of between 350 - 800 $Tg\ yr^{-1}$ (Guenther et al., 2012; Sindelarova et al., 2014). Globally, isoprene is predominately emitted from biogenic sources, but anthropogenic sources become increasingly important in urban areas especially at night (Borbon et al., 2001; Hsieh et al., 2017; Khan et al., 2018a; Mishra and Sinha, 2020; Sahu et al., 2017; Sahu and Saxena, 2015). Monoterpenes are another important BSOA precursor, with annual global emissions estimates of between 89 and 177 $Tg\ yr^{-1}$ (Guenther et al.,

86   2012; Sindelarova et al., 2014). Monoterpenes while mainly biogenic, are also emitted from
87   anthropogenic sources such as biomass burning, cooking and fragranced consumer products (Cheng
88   et al., 2018; Gkatzelis et al., 2021; Panopoulou et al., 2020, 2021; Stewart et al., 2021b, 2021c; Zhang
89   et al., 2020).

90   Numerous studies have identified and quantified molecular level markers from isoprene and
91   monoterpenes, especially in the Southeastern-US and China (Brüggemann et al., 2019; Bryant et al.,
92   2020, 2021; Hettiyadura et al., 2019; Huang et al., 2016; Rattanavaraha et al., 2016b; Wang et al.,
93   2016, 2018a; Yee et al., 2020). The complex sources of isoprene and monoterpenes in highly
94   polluted urban areas make source identification difficult. As such, the SOA markers in this study will
95   be referred to as originating from isoprene or monoterpenes, but the emissions are likely from a
96   mixture of biogenic and anthropogenic sources as discussed previously. (Cash et al., 2021b; Nelson
97   et al., 2021)

98   Recent studies have started to focus on anthropogenic-biogenic interactions, whereby
99   anthropogenic pollutants such as NO_x and sulfate enhance the formation of biogenically derived SOA
100   species. Increased NO or NO_2 concentrations can lead to higher organonitrate (ON) or nitrooxy-
101   organosulfate (NOS) concentrations through RO_2 + NO or VOC + NO_3 pathways.(Morales et al., 2021;
102   Takeuchi and Ng, 2019) Inorganic sulfate formed from the oxidation of SO_2 plays a pivotal role in OS
103   and NOS formation (Bryant et al., 2020; Budisulistiorini et al., 2015; Glasius et al., 2018; Hettiyadura
104   et al., 2019; Hoyle et al., 2011; Xu et al., 2015). Sulfate allows the acid-catalysed uptake of gas phase
105   oxidation products into the particle phase. Both chamber and ambient studies have shown the direct
106   link between sulfate and OS concentrations (Brüggemann et al., 2020a; Bryant et al., 2020;
107   Budisulistiorini et al., 2015; Gaston et al., 2014; Lin et al., 2012; Riva et al., 2019; Surratt et al.,
108   2008a; Xu et al., 2015). Yee et al., (2020) highlighted markers from both the high/low-NO isoprene
109   oxidation pathways correlated linearly with sulfate over a large range of sulfate concentrations (0.01
110   – 10 μg m^{-3}) across central Amazonia during the wet and dry seasons and in the SE-US summer. They
111   conclude that the majority of isoprene oxidation products in pre-industrial settings are still expected
112   to be in the form of isoprene OS (OSi), suggesting that they cannot be thought of as purely a
113   biogenic-anthropogenic product (Yee et al., 2020).

114   In this study, offline $PM_{2.5}$ filter samples were collected across two campaigns (pre and post-
115   monsoon) in central Delhi, alongside a comprehensive suite of gas and aerosol atmospheric
116   pollutant measurements. Filters were analysed using ultra-high performance liquid chromatography
117   tandem mass spectrometry and isoprene and monoterpene OS/NOS markers identified and
118   quantified. Isoprene and monoterpene emissions were observed to correlate strongly to
119   anthropogenic markers, suggesting a mixed anthropogenic/biogenic sources of these VOCs. OSi
120   species showed strong seasonality and strong correlations to particulate sulfate. NOS species
121   showed strong nocturnal enhancements, likely due to nitrate radical chemistry. This study is the first
122   molecular level particle phase analysis of OS and NOS markers from isoprene and monoterpenes in
123   Delhi and aims to improve our understanding of the sources of isoprene and monoterpene SOA
124   markers and their formation pathways in extremely polluted urban environments.

125   **2.Experimental**

126   **2.1 Filter collection and site information**

127   $PM_{2.5}$ filter samples were collected as part of the Air Pollution and Human Health (APHH)-India
128   campaign, at the Indira Gandhi Delhi Technical University for Women in New Delhi, India, (28°39'55"
129   N 77°13'56" E). The site is situated inside the third ring road which caters to huge volumes of traffic,

130 with a major road to the east, between the site and the Yamuna River. Two train stations are located
131 to the south and southwest of the site, and there are several green spaces locally in all
132 directions.(Nelson et al., 2021; Stewart et al., 2021c) Filters were collected during two field
133 campaigns in 2018. The first campaign was during the pre-monsoon period, with 35 filters were
134 collected between 28/05/2018 and 05/06/2018. The second campaign during the post-monsoon
135 period, 108 filters were collected between 09/10/2018 and 6/11/2018. Quartz filters (Whatman
136 QMA, 10" by 8") were pre-baked at 550 ^{o}C for 5 hours and wrapped in foil before use. Samples were
137 collected using an HiVol sampler (Ecotech 3000, Victoria Australia) with selective PM$_{2.5}$ inlet at a flow
138 rate of 1.33 m^3 min^{-1}. Once collected, filters were stored in foil at -20 ^{o}C before, during and after
139 transport for UK based analysis.

2.2 Filter extraction

141 Using a standard square filter cutter, a section of filter was taken with an area of 30.25 cm^2 which
142 was then cut into roughly 1 cm^2 pieces and placed in a 20 mL glass vial. Next, 8 mL of LC-MS grade
143 methanol (MeOH, Optima, Fisher Chemical, USA) was added to the sample and sonicated for 45 min.
144 Ice packs were used to keep the bath temperature below room temperature, with the water
145 swapped mid-way through. Using a 5 mL plastic syringe, the MeOH extract was then pushed through
146 a 0.22 μm filter (Millipore) into another sample vial. An additional 2 mL (2 x 1 mL) of MeOH was
147 added to the filter sample, and then extracted through the filter to give a combined extract ~ 10mL.
148 This extract was then reduced to dryness using a Genevac solvent evaporator under vacuum. The dry
149 sample was then reconstituted in 50:50 MeOH:H$_2$O (Optima, Fisher Chemical, USA) for analysis
150 (Bryant et al., 2020; Spolnik et al., 2018). Extraction efficiencies of 2-methyl-glyceric acid (2-MG-OS)
151 and camphorsulfonic acid were determined using authentic standards spiked onto a pre-baked clean
152 filter and recoveries were calculated to be 71 % and 99 % respectively.

2.3 Ultra-high performance liquid chromatography tandem mass spectrometry (UHPLC-MS^2)

154 The extracted fractions of the filter samples were analysed using an Ultimate 3000 UHPLC (Thermo
155 Scientific, USA) coupled to a Q-Exactive Orbitrap MS (Thermo Fisher Scientific, USA) using data
156 dependent tandem mass spectrometry (ddMS^2) with heated electrospray ionization source (HESI).
157 The UHPLC method uses a reversed-phase 5 μm, 4.6 mm × 100 mm, polar end capped Accucore
158 column (Thermo Scientific, UK) held at 40 °C. The mobile phase consisted of water (A, optima grade)
159 and methanol (B, optima grade) both with 0.1 % (v/v) of formic acid (98 % purity, Acros Organics).
160 Gradient elution was used, starting at 90 % (A) with a 1-minute post-injection hold, decreasing to 10
161 % (A) at 26 minutes, returning to the starting mobile phase conditions at 28 minutes, followed by a
162 2-minute hold allowing the re-equilibration of the column. The flow rate was set to 0.3 mL min^{-1}. A
163 sample injection volume of 4 μL was used. The capillary and auxiliary gas heater temperatures were
164 set to 320 °C, with a sheath gas flow rate of 45 (arb.) and an auxiliary gas flow rate of 20 (arb.).
165 Spectra were acquired in the negative ionization mode with a scan range of mass-to-charge (*m/z*) 50
166 to 750, with a mass resolution of 140,000. Tandem mass spectrometry was performed using higher-
167 energy collision dissociation with a stepped normalized collision energy of 10,45 and 60. The
168 isolation window was set to *m/z* 2.0 with a loop count of 10, selecting the 10 most abundant species
169 for fragmentation in each scan.

170 A mass spectral library was built using the compound database function in Tracefinder 4.1 General
171 Quan software (Thermo Fisher Scientific, USA). To build the library, compounds from previous
172 studies (Chan et al., 2010; Nestorowicz et al., 2018; Ng et al., 2008; Riva et al., 2016b; Schindelka et
173 al., 2013; Surratt et al., 2008a) were searched for in an afternoon and a night-time filter sample
174 extract analysis using the Xcalibur software. Further details can be found in Bryant et al., 2021 and

175 the SI. Isoprene OS and NOS markers were quantified using authentic standards of 2-MG-OS and 2-
176 methyl tetrol OS (2-MT-OS) with later eluting monoterpene OS and NOS quantified using
177 camphorsulfonic acid. Standards were run across a 9-point calibration curve (2 ppm – 7.8ppb, R^2 >
178 0.99) More details about the method can be found in Bryant et al., 2021. Overall uncertainties
179 associated with calibrations, proxy standards and matrix effects were estimated. The uncertainties
180 associated with 2-MG-OS and 2-MT-OS were calculated to be 58.9 % and 37.6 % respectively, mainly
181 due to the large uncertainties in the matrix correction factors. Isoprene SOA markers quantified by
182 the average of 2-MT-OS and 2-MG-OS calibrations have an associated uncertainty of 69.9 %. For
183 monoterpene SOA species which were quantified by camphorsulfonic acid, the associated
184 uncertainty is estimated to be 24.8 %.

185

186 **2.4 Supplementary measurements**

187 A suite of complementary measurements were made alongside the filter collection including
188 VOCs(Stewart et al., 2021c), oxygenated-VOCs, NO_x, CO, O_3, SO_2, HONO, photolysis rates and
189 measurements of PM_1 non-refractory aerosol chemical components with a high resolution Aerosol
190 Mass Spectrometer (HR-AMS). Detailed instrument descriptions can be found in Nelson et al.,
191 (2021). Briefly, VOCs and oxygenated-VOCs were measured via two gas-chromatography (GC)
192 instruments (DC-GS-FID and GC-GC-FID). NO_x was measured via a dual channel chemiluminescence
193 analyser with fitted with a blue light converter for NO_2 (Air Quality Designs Inc., Colorado) alongside
194 CO which was measured with a resonance fluorescent instrument (Model Al5002, Aerolaser GmbH,
195 Germany). O_3 was measured as outlined by Squires et al., (2020) using an ozone analyser (49i,
196 Thermo Scientific). SO_2 was measured using a 43i SO_2 analyser (Thermo scientific). High-resolution
197 aerosol mass spectrometry measurements were conducted as outlined in Cash et al., (2021). Ion
198 chromatography measurements were undertaken by the experimental approach outlined by Xu et
199 al., (2020) as part of an intercomparison study. Briefly, filter cuttings were taken from the filter and
200 extracted ultrasonically for 30 mins in 10 mL of ultrapure water and then filtered before analysis (Xu
201 et al., 2020).

202 Meteorology data was downloaded from the NOAA Integrated Surface Database via the Worldmet R
203 package for the Indira Gandhi International Airport (code: 421810-99999) (Carslaw, D ., accessed:
204 2021). The planetary boundary layer height (PBLH) was obtained from the ERA5 (ECMWF ReAnalysis
205 5) data product at 0.25° resolution in 1-hour time steps at the position Lat 28.625˚, Lon. 77.25˚. The
206 data for both campaigns was then selected between the start time of the first filter of that
207 campaign, and the end time of the last filter of the same campaign.

208 **3. Results**

209 **3.1 Meteorology**

210 The time series for temperature, RH, planetary boundary layer height (PBLH) and ventilation
211 coefficient (VC) across the pre- and post-monsoon campaigns are shown in Figure S1. For the pre-
212 monsoon campaign, the average air temperature was (35.8 ± 4.5) °C compared to (24.7 ± 4.6) °C in
213 the post-monsoon campaign (Table S2). The pre-monsoon campaign also showed higher average
214 wind speeds, with an average of (3.8 ± 1.4) ms^{-1}, compared to (1.7 ± 1.3) ms $^{-1}$ in the post-monsoon
215 campaign. The average RH of the pre- and post-monsoon were (39.4 ± 13.6) % and (57.3 ± 16.6) %
216 respectively, both showing similar diurnals with a minimum around mid-morning and nocturnal
217 maximum (Figure S2). The PBLH shows a similar diurnal between the two campaigns, with the
218 nocturnal boundary layer breaking down around 06:00-07:00 with a midday peak, before re-

219 establishing the nocturnal boundary layer around 19:00. The pre-monsoon PBLH has an average
220 maximum of ~2400 m compared to post-monsoon ~1700 m and a minimum of 270 m compared to
221 52 m (Figure S2). The ventilation coefficient (VC = wind speed x PBLH) has been used previously to
222 identify periods of adverse meteorological conditions and gives an idea of how stagnant atmospheric
223 conditions are and the general role of the atmosphere in the dilution of species. (Gani et al., 2019)
224 As shown in Figure S1, the conditions during the post-monsoon campaign were much more stagnant
225 than the pre-monsoon campaign. The VC was on average 4.5 times higher during the pre-monsoon
226 campaign compared to the post-monsoon campaign (Table S2) in line with previous studies (Gani et
227 al., 2019; Saha et al., 2019). The more stagnant conditions during the post-monsoon campaign likely
228 traps nocturnal emissions and their reaction products close to the surface, allowing for a significant
229 build-up of concentrations.

230 **3.2 Gas phase observations**

231 Time series of the observed mixing ratios (ppbv) of NO, NO_2 and O_3 are shown in Figure 1, for the
232 pre- and post-monsoon campaigns. The campaign averaged diurnal profiles are shown in Figure S3
233 and the mean, median and maximum mixing ratios are given in Table S2. It should be noted that only
234 one week of data was available for the pre-monsoon period. During the post-monsoon campaign,
235 extremely high mixing ratios of NO were observed with a campaign maximum mixing ratio of ~870
236 ppbv during the early morning of the 1st of November. During the early part of the pre-monsoon
237 campaign, a large enhancement in NO was observed with mixing ratios around 400 ppbv (Figure S4),
238 followed by significantly lower concentrations throughout the rest of the campaign. The campaign-
239 average NO diurnal profile shows very high NO mixing ratios at night (pre-: ~ 50 ppbv, post-: ~300
240 ppbv), with low afternoon mixing ratios < 2 ppbv due to ozone titration. These high NO
241 concentrations at night likely reduce any night-time chemistry through reactions with NO_3 radicals
242 and ozone. NO_2 during the pre-monsoon was observed to increase as the boundary layer reduced in
243 the late afternoon, with a mid-afternoon minimum. During the post-monsoon, a double peak in
244 concentrations was observed, in line with increasing ozone in the morning, and increasing NO in the
245 afternoon. Ozone showed a strong diurnal variation across both campaigns, with average afternoon
246 mixing ratios ~ 75 ppbv with pre- and post-monsoon maximums of 182 ppbv and 134 ppbv
247 respectively. Night-time O_3 concentrations were significantly higher during the pre-monsoon
248 campaign, likely due to the significantly lower NO concentrations.

249 **3.3 Particle phase observations**

250 The sampling site was heavily polluted in terms of particulate matter. The mean ± σ $PM_{2.5}$
251 concentration (Table S2) during the pre-monsoon campaign was (141 ± 31) µg m^{-3} with a spike in
252 concentrations of 672 µg m^{-3} on the 01/6/2018 at 21:00 (Figure 1). The diurnal (Figure S5) shows
253 concentrations generally flat throughout the day. During the post-monsoon campaign, the average
254 $PM_{2.5}$ concentration was higher at (182 ± 94) µg m^{-3}, with a spike in concentrations of 695 µg m^{-3} at
255 the end of the campaign (Figure 1). The diurnal shows a mid-afternoon minimum with high morning
256 and night concentrations. HR-AMS was used to measure the PM_1 sulfate and total organics.
257 Campaign averaged total organics concentrations were approximately double in the post-monsoon
258 (48.7 ± 35.4) µg m^{-3} compared to the pre-monsoon (19.8 ± 13.7) µg m^{-3}. During the pre-monsoon
259 campaign, concentrations are generally flat throughout the day, with an increase in the late
260 afternoon, likely as the boundary layer decreases (Figure S5). During the post-monsoon, a much
261 more prominent diurnal is observed, with a mid-day minimum and high night-time concentrations.
262 This diurnal is likely driven by boundary layer conditions. Sulfate averaged (7.5 ± 1.8) µg m^{-3} during
263 the pre-monsoon campaign, with slightly lower average concentrations observed in the post-

264   monsoon: (5.6 ± 2.7) μg m^{-3} as shown in Figure S5. The sulfate diurnal variations are similar to those
265   of the organic aerosol.

266

267

268

269

270
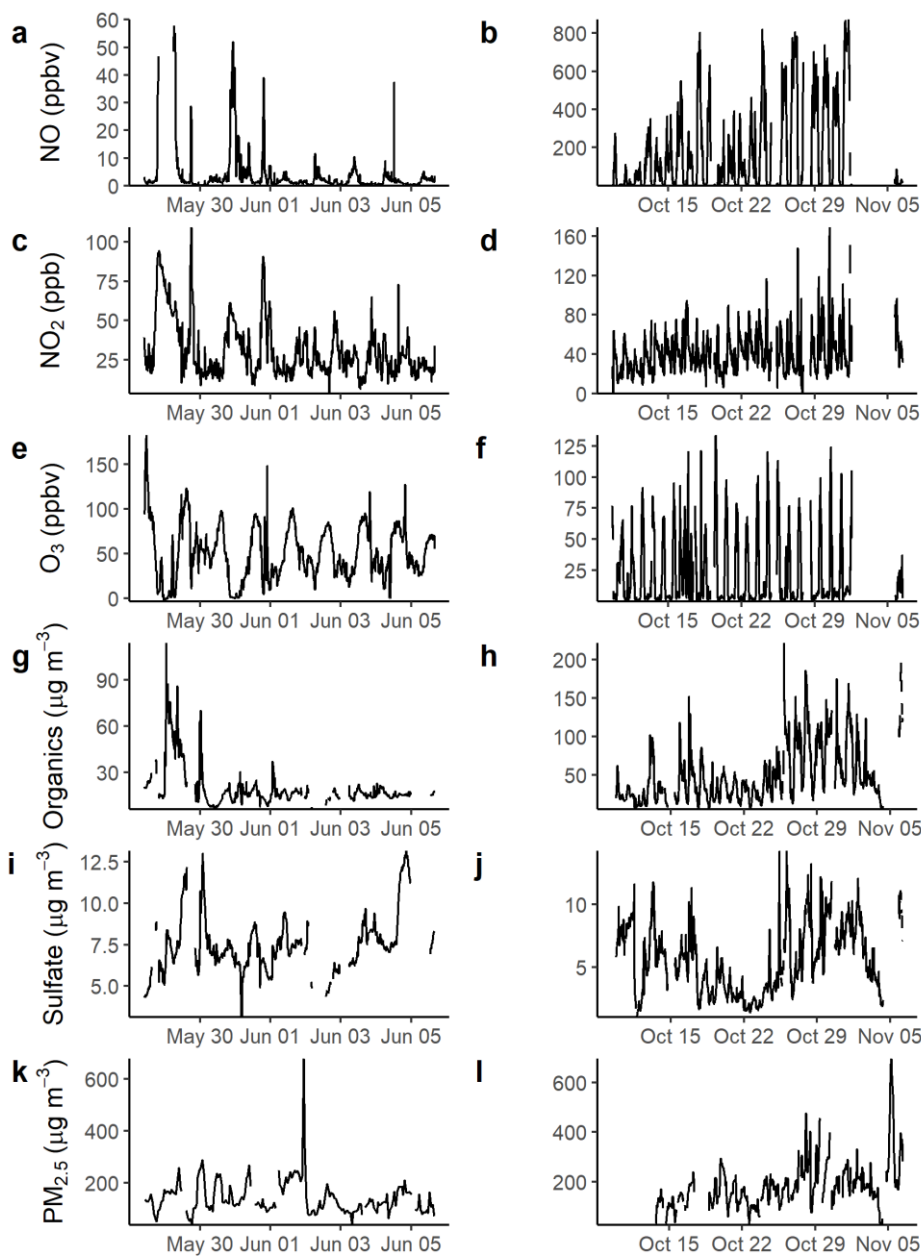
271

272

273

274

275

276

277

278

279

280

281

282

283

285

286

287

288

289

290

291

292

293   Figure 1. Time series of pollutants across the pre- (a,c,e,g,i) and post-monsoon (b,d,f,h,j)
294   campaigns. During the pre-monsoon, NO concentrations were filters to below 60 ppbv, due to
a large enhancement in concentrations at the start of the campaign, the full time series is
shown in Figure S4. NO, NO$_2$, O$_3$ and HR-AMS – SO$_4^{2-}$ were averaged to 15 minutes. PM$_{2.5}$ was
measured hourly.

3.4 Isoprene and monoterpene measurements

Isoprene was measured hourly using gas-chromatography with flame-ionisation-detection (GC-FID) across the two campaigns (Nelson et al., 2021), with the time series shown in Figure 2. The time series highlights similar diurnal variability each day, driven by biogenic emissions. Figure 3 shows the average diurnal profiles of isoprene during pre-monsoon (a) and post-monsoon (b). The mean isoprene mixing ratios were (1.22 ± 1.28) ppbv and (0.93 ± 0.65) ppbv, with maximum isoprene mixing ratios of 4.6 ppbv and 6.6 ppbv across the pre- and post-monsoon, respectively. This is in the same range as measured in Beijing (winter mean: (1.21 ± 1.03) ppbv, summer mean: (0.56 ± 0.55) ppbv, Acton et al., (2020)), Guangzhou (year round (1.14) ppbv) (Zou et al., 2019) and Taipei (summer daytime: (1.26) ppbv, autumn daytime: (0.38) ppbv) (Wang et al., 2013). The diurnal variability observed in the pre-monsoon period corresponds to a typical biogenic emission driven profile, with a rapid increase of isoprene around 05:00, reaching a peak around or after midday, before a nocturnal minimum. Figure 3 indicates that average daytime peak isoprene mixing ratios during the pre-monsoon campaign were roughly double that of the post-monsoon campaign. In contrast, average nocturnal mixing ratios of isoprene were 5 times higher in the post-monsoon compared to the pre-monsoon ((0.65 ± 0.43) ppbv versus (0.13 ± 0.18) ppbv). In the post-monsoon campaign, isoprene mixing ratios show a strong biogenic emission driven diurnal profile at the start of the campaign. However, towards the end of the post monsoon measurement period, the isoprene mixing ratios become less variable with a high mixing ratio maintained overnight (Figure 2). This is potentially due to more stagnant conditions as observed by the VC in Figure S1.

332

333

334
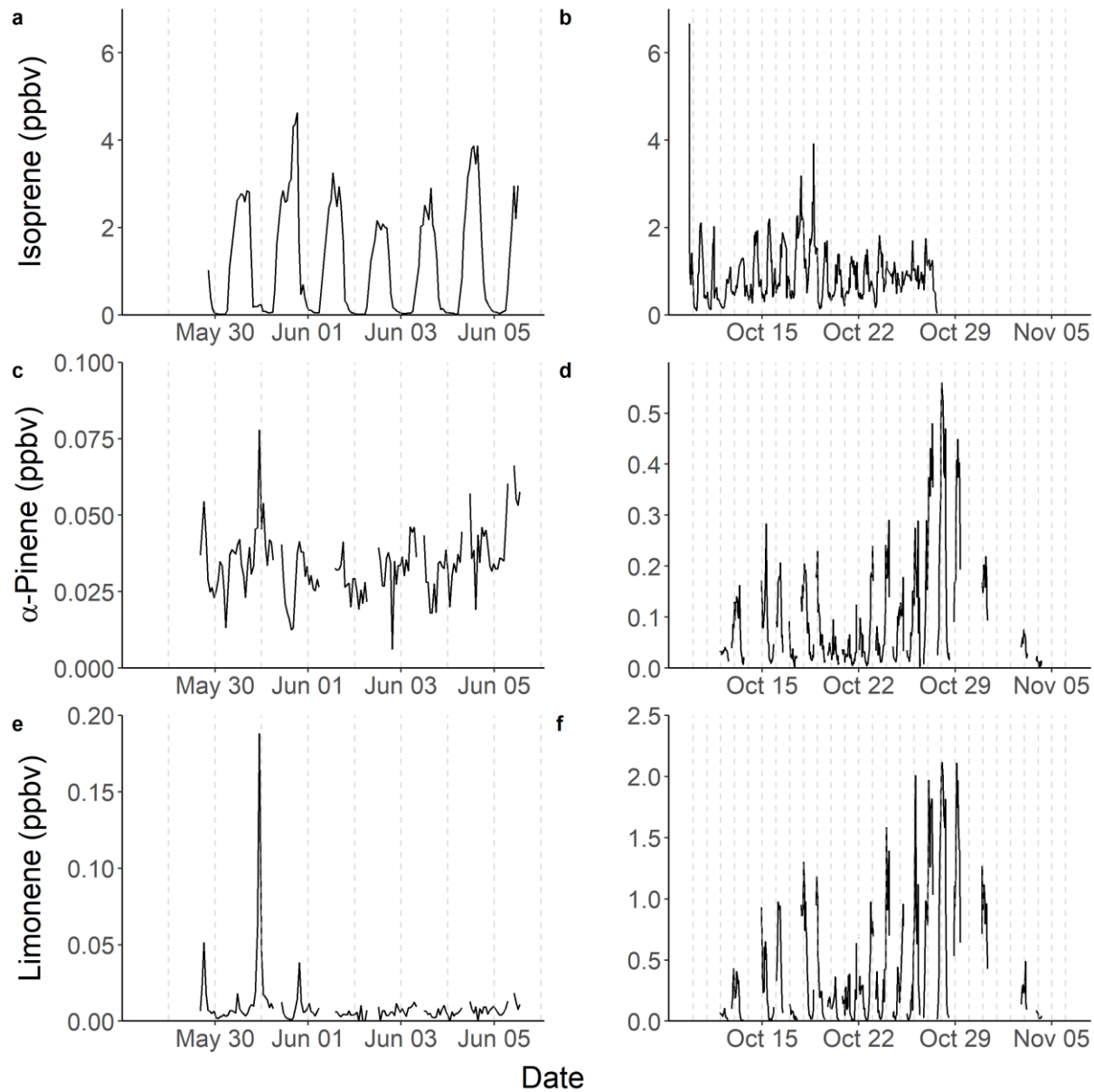
Figure 2. Time series across the pre- (left) and post-monsoon (right) campaigns of Isoprene (a,b), α-pinene (c,d), limonene (d,e). The vertical dotted lines represent midnight for each day.

A recent study in Delhi averaged across post-monsoon, summer and winter campaigns found that at vegetative sites biogenic isoprene contributed on average 92 - 96 % to the total isoprene, while at traffic dominated sites only 30 – 39 % of isoprene was from biogenic sources (Kashyap et al., 2019). This is similar to the contributions of biogenic isoprene (40 %) to total isoprene mixing ratios at the traffic dominated Marylebone Road London site.(Khan et al., 2018a) To gain some understanding of

the sources of isoprene at our site in Delhi, the observed concentrations of isoprene were correlated
to CO, which is an anthropogenic combustion tracer (Figure 5) similar to previous studies.(Khan et
al., 2018a; Wagner and Kuttler, 2014) The isoprene concentrations were split between night and day
(pre-monsoon; night: 19:00 – 05:00 h, day 05:00 – 19:00 h, post-monsoon; night: 17:00-06:00 h, day:
06:00-17:00 h), based on the observed isoprene diurnals as shown in Figure 3. Isoprene correlated
strongly with CO during the night across both campaigns (pre-monsoon: R^2= 0.69, post-monsoon:
R^2= 0.81), but no correlation was observed during the day ($R^2 < 0.1$). This suggests that daytime
isoprene is predominantly from biogenic sources, although a small amount will be from
anthropogenic sources, and that nocturnal isoprene is emitted from anthropogenic sources, as seen
in other locations. (Khan et al., 2018b; Panopoulou et al., 2020; Wang et al., 2013) The night-time
isoprene mixing ratios (pre-monsoon: (0.13 ± 0.18) ppbv, post-monsoon: (0.65 ± 0.43) ppbv) were
substantially higher than measured previously in Beijing and London (<50pptv, (Bryant et al., 2020;
Khan et al., 2018b)), but pre-monsoon concentrations were similar to those observed at night in
Taipei (0.19 ppbv)(Wang et al., 2013). The high night-time concentrations during the post-monsoon
period, towards the end of October are also likely influenced by the formation of a very low
boundary layer, trapping pollutants near the surface, affecting all species similarly. An increase in
biomass burning may also be a factor. Therefore, during the post-monsoon campaign a significant
amount of isoprene oxidation products will be of anthropogenic origin.
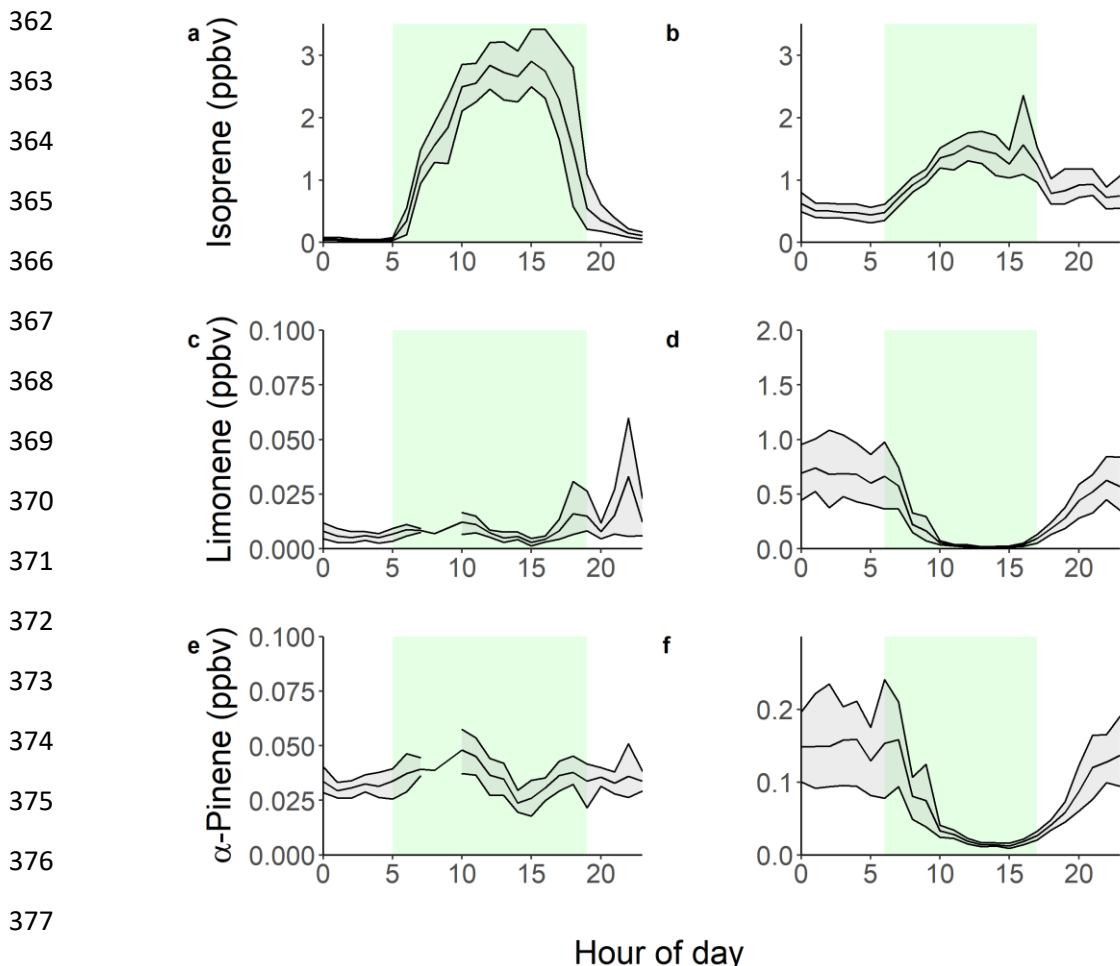
Figure 3. Diurnal variations across the pre (left) and post-monsoon (right)
campaigns of Isoprene (a,b), limonene (c,d) and α-pinene (e,f). The grey
shaded area represents the 95 % confidence interval. The green shaded area
represents the times driven by biogenic emissions, as defined by the isoprene
diurnals.

381

382

383

384 Several monoterpenes were measured using GCxGC-MS. The time series of two monoterpenes,
385 limonene and α-pinene, are shown in Figure 2. The α-pinene mixing ratio averaged (0.034 ± 0.011)
386 ppbv during the pre-monsoon and (0.10 ± 0.11) ppbv during the post monsoon periods. This is in
387 comparison to limonene, which averaged (0.01 ± 0.02) ppbv and (0.42 ± 0.51) ppbv across the pre-
388 and post-monsoon campaigns, respectively. A strong diurnal variation was observed for both
389 monoterpenes during the post-monsoon, peaking during the night (Figure 3), with a midday
390 minimum. Nocturnal mixing ratios of the two monoterpenes were substantially higher during the
391 post-monsoon (Limonene: (0.59 ± 0.11) ppbv, α-pinene: (0.13 ± 0.12) ppbv) than the pre-monsoon
392 (Limonene: (0.011 ± 0.025) ppbv, α-pinene: (0.033 ± 0.009) ppbv) period. The diurnal variations across
393 both campaigns are likely driven by both emissions as well as boundary layer effects. The boundary layer effect
394 however is much stronger during the post-monsoon, with a shallower nocturnal boundary layer, as such the
395 post-monsoon period has a more pronounced diurnal.Limonene was dominated by 3 short lived spikes in
396 concentrations towards the start of the campaign (Figure 2). α-pinene concentrations generally
397 increased during the morning, before decreasing during the afternoon. Multiple monoterpenes
398 were measured concurrently using GCxGC-MS (Nelson et al., 2021; Stewart et al., 2021c). For all MT
399 species, the post monsoon period had higher mean mixing ratios, with large nocturnal
400 enhancements in mixing ratios. There are likely multiple factors leading the higher concentrations
401 during the post-monsoon, including accumulation due to boundary layer effects, a lack of nocturnal
402 radical chemistry and an increase in biomass burning (Jain et al., 2014). The average isomeric
403 speciation of the measured monoterpenes showed low variability between day and night-time
404 samples during each campaign, but significant differences were observed between the campaigns
405 (Figure 4). Higher contributions from limonene and β-ocimene were observed during the post-
406 monsoon compared to the pre-monsoon. The reason for the difference in composition is likely due
407 to differences in sources and/or sinks between the two periods.

408

409
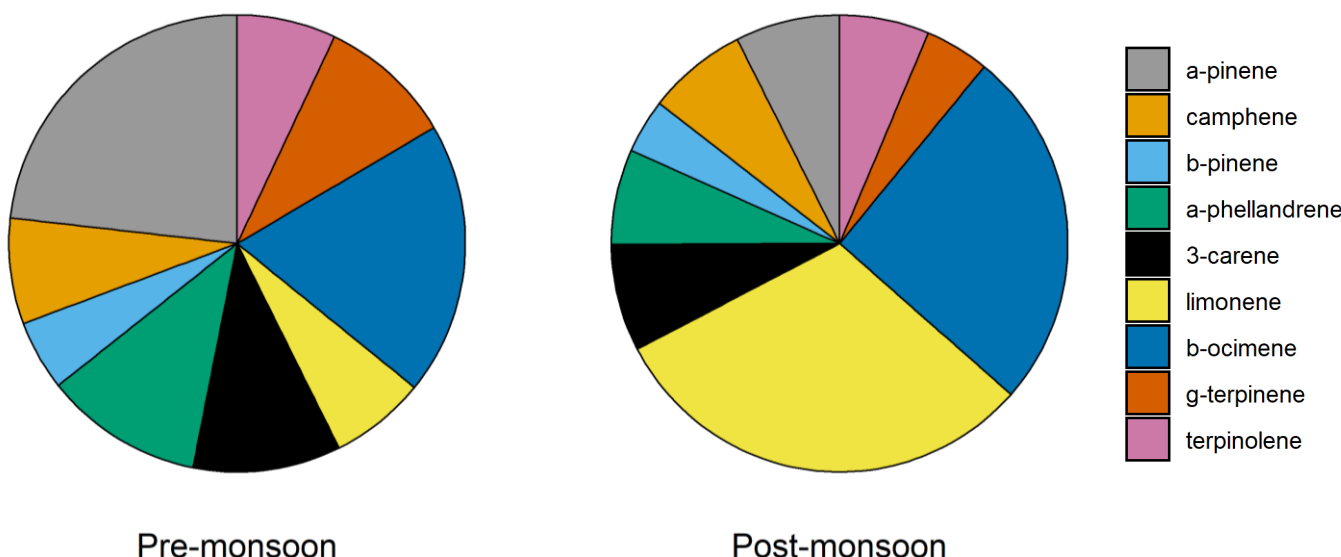
410

411

412   Figure 4. Average composition of monoterpenes across the pre-monsoon and post-monsoon
413   periods.

414

415

416

417

418

419

420

421

422   During the post-monsoon, α-pinene and limonene correlated strongly with CO during the day (α-
423   pinene; R^2 = 0.82, limonene; R^2 = 0.90) and moderately at night (α-pinene; R^2 = 0.49, limonene; R^2 =
424   0.56) as shown in Figure 5, suggesting anthropogenic sources. Other potentially important
425   anthropogenic monoterpene sources include biomass burning, cooking and the use of personal
426   care/volatile chemical products (Coggon et al., 2021; Gkatzelis et al., 2021; Hatch et al., 2019; Klein
427   et al., 2016). The shallow nocturnal boundary layers across both campaigns leads to relatively high
428   concentrations of total monoterpenes, with a maximum mixing ratio of 6 ppbv observed during the
429   post-monsoon (Stewart et al., 2021c). After sunrise, the expanding boundary layer dilutes the high
430   concentrations alongside increasing OH concentrations from photolytic sources such as the
431   photolysis of HONO and carbonyls which likely causes a rapid decrease in the monoterpene mixing
432   ratios. (Lelieveld et al., 2016)

433
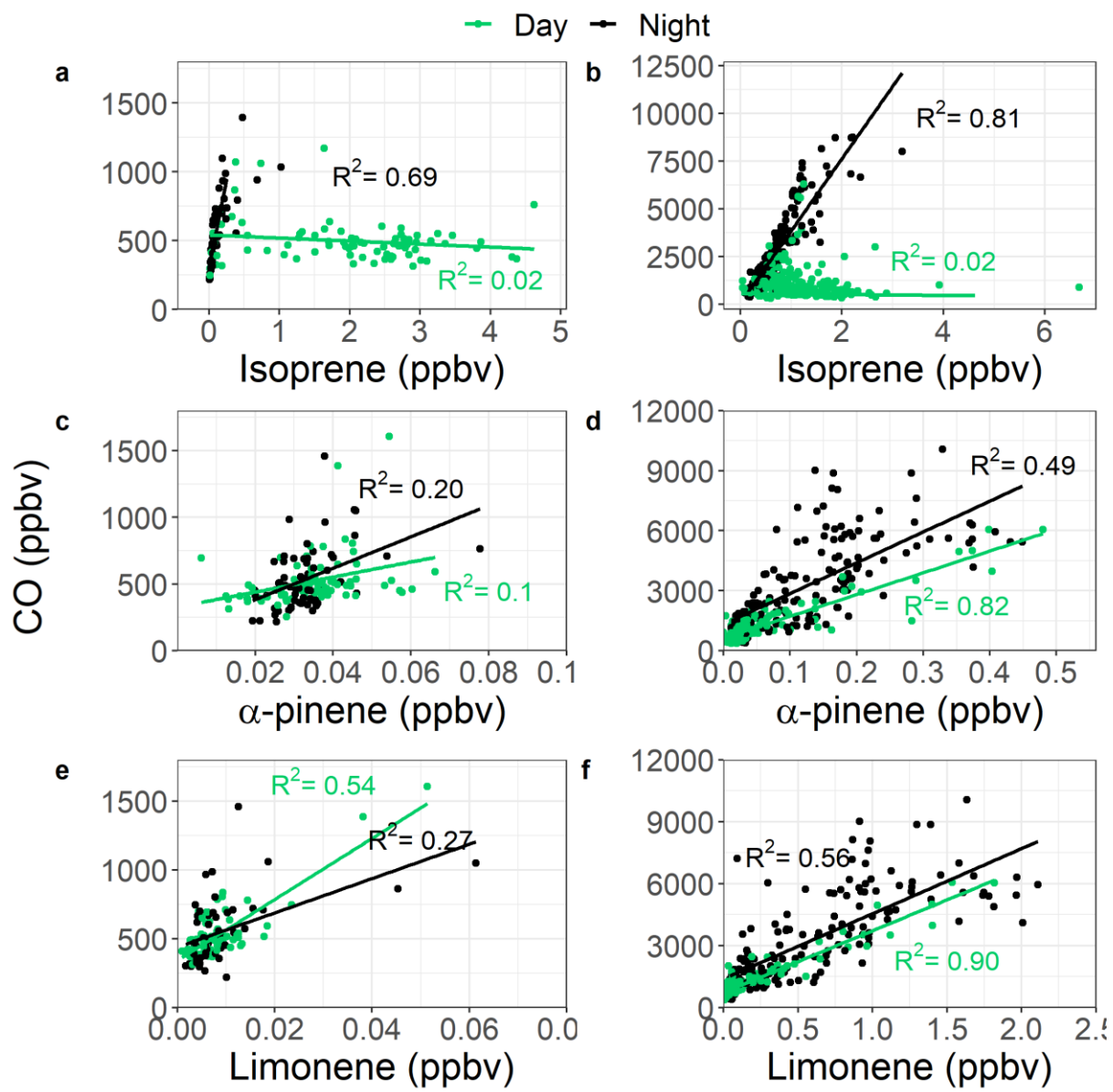
Figure 5. Correlations between Isoprene, limonene and α-pinene with CO across the pre (left) and post-monsoon (right) campaigns. The samples are split between daytime (green) and night-time (black) as defined by the Isoprene diurnals in Figure 3.

443

444

445
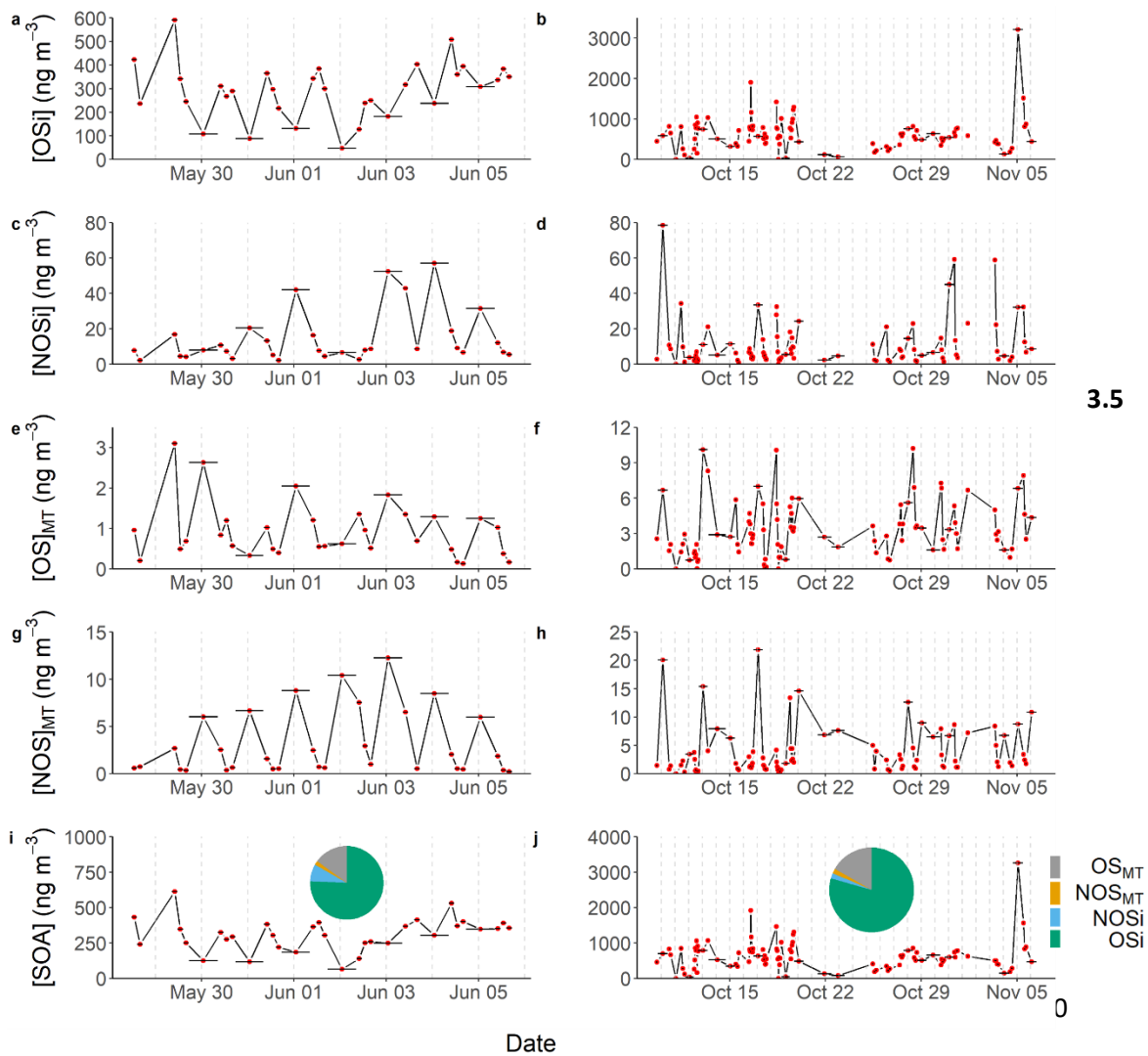
Figure 6. Time series across the pre- (left) and post-monsoon (right) campaigns of the quantified SOA tracers: OSi (a,b), NOSi (c,d), OS_{MT} (e,f), NOS_{MT} (g,h) and the sum of all SOA tracers (i,j) with the average campaign contributions. The vertical dotted lines represent midnight for each day. Only species identified in more than 40 % of the samples for each campaign were included.

465

466

Isoprene and monoterpene OS and NOS formation

At the measured concentrations, monoterpenes and isoprene are an important source of ozone and OH reactivity at this site (Nelson et al., 2021). The resultant oxidised products will also be a key source of SOA production. The UHPLC-MS^2 analysis identified and quantified 75 potential markers across four classes of SOA, isoprene OS (OSi) and NOS (NOSi) derived species and monoterpene OS (OS_{MT}) and NOS (NOS_{MT}) species. Figure 6 shows the contribution to the total quantified SOA (qSOA),

473 which consists of the time averaged sum of the four SOA classes (OSi, NOSi, OS$_{MT}$, NOS$_{MT}$), across the
474 pre- and post-monsoon campaigns. OSi species were the dominant SOA class quantified in this
475 study, contributing 75.6 % and 79.4 % of the qSOA across the pre- and post-monsoon campaigns
476 respectively. NOSi species contributed significantly more to the qSOA during the pre-monsoon (7.6
477 %) compared to the post-monsoon (2.1 %) period. Similar contributions from the monoterpene
478 derived SOA species were observed across both campaigns.

479 **3.5.1 Isoprene OS and NOS markers**

480 OSi species are predominantly formed by photo-oxidation of isoprene by OH radicals with the
481 subsequent products formed dependent on ambient NO concentrations (Wennberg et al., 2018).
482 The pathways are split into high-NO and low-NO, although the NO concentrations that constitute
483 high and low are a sliding scale depending on the amount of reactivity (defined as ([OH] x k_{OH})
484 (Newland et al., 2021). Under low-NO conditions, isoprene epoxydiol isomers (IEPOX) (Paulot et al.,
485 2009) are formed which can then undergo reactive uptake to the particle phase by acid-catalysed
486 multiphase chemistry involving inorganic sulfate, to form 2-MT-OS (Lin et al., 2012; Riva et al., 2019;
487 Surratt et al., 2010). Under high-NO conditions, 2-methyl glyceric acid is the dominant gas-phase
488 marker produced, which can undergo reactive uptake to the particle phase to form 2-MG-OS (Lin et
489 al., 2013a; Nguyen et al., 2015; Surratt et al., 2006, 2010).

490 A total of 21 potential OSi C$_{2-5}$ markers previously identified in chamber studies (Nguyen et al., 2010;
491 Riva et al., 2016a; Surratt et al., 2007, 2008b) and other ambient studies (Bryant et al., 2020;
492 Budisulistiorini et al., 2015; Hettiyadura et al., 2019; Kourtchev et al., 2016; Rattanavaraha et al.,
493 2016a; Wang et al., 2018b, 2021b) were quantified in the collected ambient samples. It should be
494 noted that several of the smaller (C$_{2-3}$) OSi tracers likely form from glyoxal, methylglyoxal and
495 hydroxyacetone as well as isoprene, and as such present a potential non-isoprene source of OSi
496 (Galloway et al., 2009; Liao et al., 2015).

497 Figure 6 shows the time series of total OSi concentrations observed across pre- (left, 5a) and post-
498 (right, 5b) monsoon campaigns. Total OSi time averaged concentrations (Table 1) were c.a. 2.3 times
499 higher during the post-monsoon (~556.6 ± 422.5 ng m^{-3}) campaign than the pre-monsoon campaign
500 (~237.8 ± 118.4 ng m^{-3}). These concentrations are similar to those observed in Beijing during summer
501 2017 (237.1 ng m^{-3}, (Bryant et al., 2020)), but higher than those observed in Shanghai in 2018 (40.4
502 ng m^{-3}) and 2019 (34.3 ng m^{-3}) (Wang et al., 2021b). As previously discussed, OSi species have been
503 shown to form via the gas-phase photo-oxidation of isoprene, with the reactive uptake of the
504 oxidised species into the particulate phase via sulfate (Lin et al., 2013a; Surratt et al., 2010).
505 Recently, a heterogeneous photo-oxidation pathway from 2-MT-OS (C$_5$H$_{12}$O$_7$S) to several OSi species
506 was proposed, including C$_5$H$_{10}$O$_7$S, C$_5$H$_8$O$_7$S, C$_5$H$_{12}$O$_8$S, C$_5$H$_{10}$O$_8$S and C$_4$H$_8$O$_7$S (Chen et al., 2020). 2-
507 MT-OS showed moderate correlations (pre-monsoon : R^2 = 0.52-0.72, post-monsoon: R^2 = 0.14-0.35)
508 with these OSi tracers that were lower than observed in Beijing summer (R^2 = 0.83-0.92) (Bryant et
509 al., 2020). These correlations could suggest that this is a more common formation route in pre-
510 monsoon Delhi, than in post-monsoon. However, the correlations could also be driven by the
511 common pathways between the OSi species, with the reactive uptake of gas phase intermediates via
512 sulfate reactions. The lower correlations during the post-monsoon could be due to increased
513 influences of anthropogenic sources coupled to the stagnant conditions.

514 Figure 7 shows the binned OSi concentrations for each filter collection time across the pre- and post-
515 monsoon campaigns to create a partial diurnal profile. During the pre-monsoon, the daily variation
516 in OSi concentrations was much clearer, with day-time maxima and nocturnal minima, which are in
517 line with daily peak isoprene (Figure 3) and OH radical concentrations. The highest observed OSi

518 concentrations during the pre-monsoon were ~ 600 ng m^{-3}, which occurred at the start of the
519 campaign. High isoprene concentrations may have been the cause, but unfortunately isoprene
520 measurements were not available during this period to confirm. However, high OSi concentrations
521 also occurred when particulate inorganic sulfate concentrations were at their highest (Figure S6),
522 while sulfate measured via the HR-AMS was also high during this period (Figure 1). During the post-
523 monsoon, although a similar diurnal pattern was observed, the variation was less pronounced, with
524 higher OSi concentrations observed at the start and end of the campaign (Figure 6). Due to the
525 secondary nature of sulfate, the sulfate concentrations are less likely to be influenced by the
526 boundary layer effects, compared to directly emitted VOCs. The low OSi concentrations during the
527 middle of the campaign, coincide with lower isoprene and inorganic sulfate concentrations, but also
528 low VC values, suggesting more stagnant conditions.

529 The sum of OSi species across all filters sampled showed a variable correlation with particulate
530 sulfate across both campaigns. The pre-monsoon correlation was similar to those observed in
531 Beijing, Guangzhou and the SE-US (R^2: 0.55)(Bryant et al., 2020, 2021; Budisulistiorini et al., 2015;
532 Rattanavaraha et al., 2016a) while the post-monsoon was significantly weaker (R^2: 0.28). However, a
533 clear relationship between OSi tracers and inorganic sulfate can be seen in Figure 8 across both
534 campaigns, where the highest OSi concentrations occurred under the highest particulate sulfate
535 concentrations. During the post-monsoon campaign, OSi concentrations levelled off at high sulfate
536 concentrations. In the pre-monsoon this levelling off is not observed, potentially due to the lower
537 number of samples. The high concentrations of organics measured by the HR-AMS (Table S2) during
538 the post-monsoon (48.7 ± 35.4) μg m^{-3} compared to the pre-monsoon (19.8 ± 13.7) μg m^{-3}, suggests
539 the reactive uptake of the gaseous OSi intermediates to the aerosol phase may be limited due to
540 extensive organic coatings on the sulfate aerosol. Multiple studies have now shown that organic
541 coatings on sulfate aerosol can limit the reactive uptake of IEPOX, suggesting the pre-monsoon is
542 volume limited but the post-monsoon is diffusion limited. (Gaston et al., 2014; Lin et al., 2014; Riva
543 et al., 2016c)

544 Isoprene NOS (NOSi) have been shown to be produced by photo-oxidation in the presence of NO
545 and from NO$_3$ oxidation chemistry (Hamilton et al., 2021; Ng et al., 2017; Surratt et al., 2008b). Ten
546 different NOSi tracers were screened for across the two campaigns, with eight identified in the pre-
547 monsoon and ten in the post-monsoon. These tracers included: mono-nitrated ($C_5H_9O_{10}NS$,
548 $C_5H_{11}O_9NS$, $C_5H_{11}O_8NS$), di-nitrated ($C_5H_{10}O_{11}N_2S$), and tri-nitrated ($C_5H_9O_{13}N_3S$) species. These tracers
549 have been identified previously in China (Bryant et al., 2020, 2021; Hamilton et al., 2021; Wang et
550 al., 2018b, 2021b). Unlike the OSi tracers, total NOSi concentrations were on average higher during
551 the pre-monsoon (32.6 ± 19.9) ng m^{-3} compared to the post-monsoon (20.2 ± 13.3) ng m^{-3}. This is
552 likely due to extremely high night-time NO concentrations during the post-monsoon quenching NO$_3$
553 radicals, limiting the isoprene + NO$_3$ pathway. The NOSi time series and diurnal shown in Figures 5
554 and 6 respectively highlight the strong nocturnal enhancements in concentrations during the pre-
555 monsoon, suggesting isoprene + NO$_3$ formation pathway is dominant. Due to the long sampling time,
556 it is likely that these species are forming in the early evening as NO$_3$ oxidation becomes more
557 competitive with OH, while isoprene concentrations are still relatively high. During the post-
558 monsoon, NOSi concentrations were highest at night and the early morning. The high morning
559 concentrations could be due to non-local sources mixing down as the shallow night-time boundary
560 layer breaks down. Ideally, future work in Delhi or India should focus on the measurements of
561 radicals and OH reactivity (k_{OH}), in order to improve our understanding of the chemistry occurring in
562 extremely polluted environments. A large spike in NOS$_i$ concentrations is observed at the start of the
563 post-monsoon campaign, which was not observed for the OS$_i$ tracers, this coincides with lower NO
564 concentrations than the rest of the post-monsoon campaign, reducing the NO$_3$ quenching by NO,

565 allowing for more isoprene + NO₃ oxidation. The NOSi species did not correlate towards particulate
566 sulfate ($R^2 < 0.2$) across either campaign, suggesting that uptake onto sulfate is not the limiting step
567 in NOSi formation (unlike for the OSi species).

568

569

570

571

572 Filter collection time
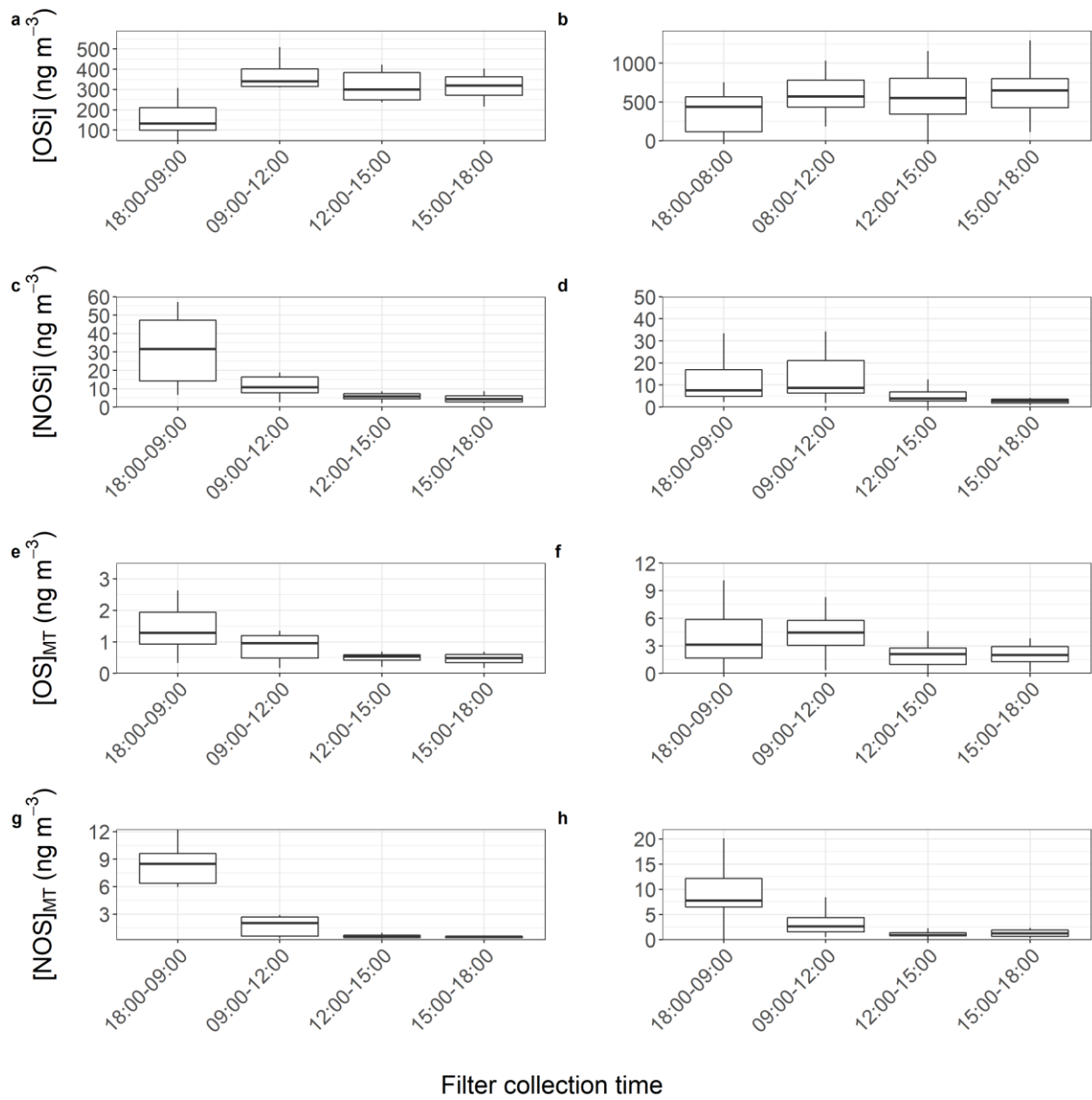
573

574 Figure 7. Partial diurnal variations from the binned concentrations of OSi, NOSi, OS$_{MT}$ and
NOS$_{MT}$ concentrations at each filter collection time across the pre (left) and post-monsoon
(right) campaigns. The lower and upper part of the box representing the 25th and 75th
percentiles, with the upper and lower lines extending no further than 1.5 times the
interquartile range of the highest and lowest values within the hinge respectively. Only
species identified in more than 40 % of the samples for each campaign were included.

Figure 8. Quantified SOA (OS_i, NOS_i, OS_{MT}, NOS_{MT}) vs inorganic sulfate concentrations across the pre- (left) and post-monsoon (right) campaigns. The lower and upper part of the box representing the 25th and 75th percentiles, with the upper and lower lines extending no further than 1.5 times the interquartile range of the highest and lowest values within the hinge respectively. Only species identified in more than 40 % of the samples for each campaign were included.
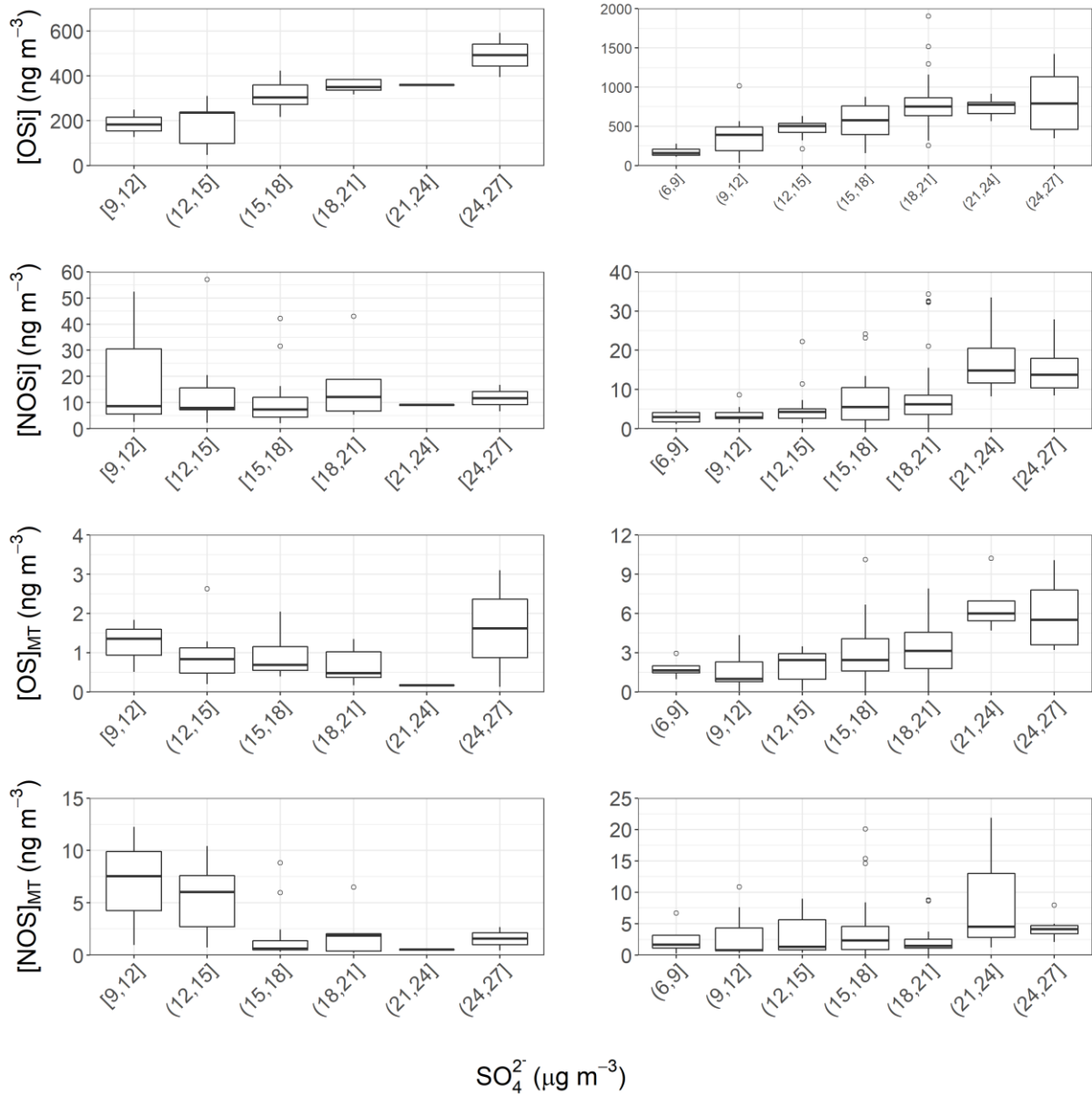
575

576

577

578

579

580

581

582

583

584

585

3.5.2 Monoterpene OS and NOS markers

Monoterpene derived OS (OS_{MT}) and NOS (NOS_{MT}) markers have also been identified from the oxidation by OH, NO_3 and O_3 in the presence of SO_2 or sulfate seed in simulation studies (Brüggemann et al., 2020b; Iinuma et al., 2007; Kleindienst et al., 2006; Surratt et al., 2008a; Zhao et al., 2018). Compared to isoprene, the ozonolysis of monoterpenes is a key degradation pathway, with higher SOA yields from ozonolysis observed when compared to isoprene (Åsa M. Jonsson et al., 2005; Atkinson and Arey, 2003; Eddingsaas et al., 2012a, 2012b; Kristensen et al., 2013; Mutzel et al., 2016; Simon et al., 2020; Zhao et al., 2015). A recent study in the SE-US suggests that the degradation of 80 % of monoterpenes at night is due to ozonolysis at that location (Zhang et al., 2018). Monoterpene derived OS and NOS species have been extensively observed, with ON contributing considerably to OA (Lee et al., 2016; Xu et al., 2015; Zhang et al., 2018). Recently NOS hydrolysis has also been shown to be a potential formation route of OS particle phase species (Darer et al., 2011; Passananti et al., 2016).

Twenty-three monoterpene-derived organosulfate (OS_{MT}) species, which have been seen previously in chamber (Surratt et al., 2008b) and ambient studies (Brüggemann et al., 2019; Wang et al., 2018b, 2021b), were identified across the pre- and post-monsoon campaigns. It should be noted that recently OS_{MT} artefacts has been shown to form when filters have been sampled without a denuder. (Brüggemann et al., 2020b). However, the strong diurnal variations of the OS_{MT} species, and lack of correlation with SO_2 suggest this process is unlikely to have contributed significantly to the OS_{MT} measured in this study. Post-monsoon concentrations were similar (3.96 ± 1.6) ng m^{-3} to the pre-monsoon (3.05 ± 1.3) ng m^{-3}, with $C_9H_{16}O_6S$ the dominant species across both campaigns, contributing on average ~ 29 % of the OS_{MT} mass. $C_9H_{16}O_6S$ has been observed in chamber studies (Surratt et al., 2008a) as well as in ambient samples in Denmark, Shanghai and Guangzhou previously(Bryant et al., 2021; Nguyen et al., 2014; Wang et al., 2017). It should be noted that the majority of the OS_{MT} were not identified in every sample, and as such only tracers which were identified in at least 40 % of the samples were examined further.

Total OS_{MT} showed a strong diurnal profile across both campaigns, peaking at night, with an afternoon minimum (Figures 5 & 6). During the pre-monsoon campaign, the highest OS_{MT} concentrations were observed during a day-time sample, coinciding with peak sulfate and NO concentrations. Both limonene and α-pinene also show peaks during this filter sampling period of ~ 0.05 ppbv. Spikes in limonene and α-pinene concentrations were also observed on the 31st of May, but OS_{MT} concentrations were much lower, likely due to the lower sulfate concentrations. During the post-monsoon campaign, nocturnal enhancements are observed (Figure 7), suggesting MT + NO_3 chemistry is important. Like the NOSi markers, higher OS_{MT} concentrations were observed during the early morning sample, likely due to a lower PBLH concentrating the markers coupled to MT+OH/O_3 occurring after sunrise in the post-monsoon. The night-time formation of the OS_{MT} species is in line with previous studies (Bryant et al., 2021), and with the diurnal variations of α-pinene and limonene, which peak at night. Previous chamber studies investigating reactions of monoterpenes with NO_3 radicals have also shown formation of OS_{MT} with the same molecular formulae as measured here (Surratt et al., 2008a).

OS_{MT} concentrations observed in Delhi are much lower than those of the OSi, similar to other studies (Hettiyadura et al., 2019; Wang et al., 2018b, 2021b). Considering the high concentrations of extremely reactive α-pinene and limonene observed during the post-monsoon period, higher OS_{MT} concentrations might be expected. One possible reason for the low OS_{MT} is the inability of OS_{MT}

630 precursor species to undergo reactive uptake into the aerosol phase under atmospherically relevant
631 acidic conditions, with chamber studies suggesting extremely acidic conditions are needed for
632 uptake to occur (Drozd et al., 2013). Delhi is characterised by large concentrations of free ammonia
633 and alkaline dust, and previous studies have highlighted that it has less acidic aerosol (pH 5.7 – 6.7,
634 Kumar et al., 2018) across the year than Beijing (pH 3.8 – 4.5, Ding et al., 2019) and the SE-US (pH 1.6
635 – 1.9, Rattanavaraha et al., 2016a).

636 Unlike the OS_{MT} species, the NOS_{MT} species ($C_{10}H_{17}NO_7S$, $C_9H_{15}NO_8S$, $C_{10}H_{17}NO_9S$, $C_9H_{15}NO_9S$,
637 $C_{10}H_{17}NO_8S$) showed strong seasonality, with pre- and post-monsoon concentrations of (7.6 ± 3.8) ng
638 m^{-3} and (17.6 ± 6.1) ng m^{-3} respectively. This is opposite to the quantified NOSi species, which
639 showed higher pre-monsoon concentrations. This is likely due to much higher post-monsoon
640 concentrations of monoterpenes. Of the NOS_{MT} species observed, $C_{10}H_{17}NO_7S$ was the most
641 abundant, contributing on average 79 % and 76 % of the NOS_{MT} concentrations across the pre- and
642 post-monsoon respectively. Previous studies have also highlighted $C_{10}H_{17}NO_7S$ to be the dominant
643 monoterpene derived sulfate containing tracer (Wang et al., 2018b). In the post-monsoon nine
644 $C_{10}H_{17}NO_7S$ isomers were observed, and seven in the pre-monsoon. The summed $C_{10}H_{17}NO_7S$
645 concentrations during the pre- (5.96 ± 3.33) ng m^{-3} and post-monsoon (13.36 ± 4.98) ng m^{-3}, are of a
646 similar magnitude to those observed in other locations as shown in Table 2. These concentrations
647 are also similar to those quantified by authentic standards across four Chinese megacities (Wang et
648 al., 2021a). Like the OS_{MT} species, some NOS_{MT} species were not identified in many of the filter
649 samples, and as such tracers which were observed in more than 40 % of the samples were summed
650 for further analysis. The NOS_{MT} pre-monsoon time series (Figure 6) shows a similar temporal profile
651 to the NOSi species, with lower concentrations during the enhancement in NO concentrations
652 (Figure S4) at the start of the campaign. NOS_{MT} showed strong diurnal variations across both
653 campaigns (Figure 7), peaking at night with lower concentrations during the afternoon, as seen
654 previously (Bryant et al., 2021; Wang et al., 2018b). Therefore, the formation of NOS_{MT} is likely
655 dominated by NO_3 radical chemistry. Both NOS_{MT} and OS_{MT} species showed limited correlation
656 towards SO_2 and particulate sulfate ($R^2 < 0.1$), indicating that although sulfate is essential to their
657 formation, sulfate availability does not control NOS_{MT} concentrations.

658

3.5.3 Contributions of total Isoprene and monoterpene OS and NOS (qSOA) to particulate mass

660 Particulate concentrations in Delhi are among the highest across the world (WHO, 2018), with
661 concentrations over 600 µg m^{-3} being observed during this study. qSOA, defined here as the sum of
662 all OSi, NOSi, OS_{MT}, and NOS_{MT} tracers quantified (including those not identified in more than 40 % of
663 the samples), was calculated to determine the total contribution these species make to particulate
664 mass in Delhi. Total oxidised organic aerosol (OOA), a proxy for SOA in PM_1, was derived from the
665 HR-AMS measurements during the pre- and post-monsoon campaigns, with averages of (19.8 ± 13.7)
666 µg m^{-3} and (48.7 ± 35.4) µg m^{-3} respectively. qSOA contributed on average (2.0 ± 0.9) % and (1.8 ±
667 1.4) % to the total OOA. Isoprene and monoterpene derived species contributed on average 83.2 %
668 and 16.8 % of qSOA across the pre-monsoon respectively compared to 81.5 % and 18.5 % during the
669 post-monsoon respectively. During certain periods qSOA contributed a maximum of 4.2 % and 6.6 %
670 to OOA during the pre- and post-monsoon, respectively. This is under the assumption that when the
671 OS and NOS species fragment in the AMS ion source they lose their sulfate and nitrate groups. This is
672 similar to the contributions made by OSi markers in Beijing to total OOA (2.2 %) (Bryant et al., 2020).
673 Previous studies in the SE-US have reported much higher contributions of isoprene species to total
674 OA. As quantified by an aerosol chemical speciation monitor, summed iSOA tracers on average
675 accounted for 9.4 % of measured OA at Look Rock, downwind of Maryville and Knoxville, but up to a

676 maximum of 28.1 % (Budisulistiorini et al., 2015). This is lower than that measured at a rural site at
677 Yorkville, Georgia with just low-NO isoprene SOA tracers accounting for between 12-19 % of total OA
678 (Lin et al., 2013b).

679 Sulfate was also measured in the PM$_1$ size range by HR-AMS, with pre- and post-monsoon mean
680 concentrations of (7.5 ± 1.8) µg m^{-3} and (5.5 ± 2.7) µg m^{-3}. The sulfate containing OS and NOS species
681 quantified in this study may fragment in the AMS to produce a sulfate signal which is not related to
682 inorganic sulfate. To estimate the contribution that sulfate contained within qSOA species could
683 make to total AMS sulfate, the quantified mass of sulfate contained within each marker was
684 calculated based on the fraction of sulfate to each marker molecular mass. For example, 2-MT-OS
685 has an accurate mass of *m/z* 216.21, meaning the percentage of 2-MT-OS mass associated with
686 sulfate is ~44 %. During the pre-monsoon campaign the qSOA sulfate accounted for on average 2.2
687 % to the total PM$_1$ sulfate, but up to 4.8 % on certain days. qSOA contributed considerably more to
688 the sulfate in the post-monsoon campaign, with an average of (6.1 ± 4.5) % with a maximum of 18.7
689 %. This finding indicates the need to consider the sources of particulate sulfate measured by the
690 AMS when calculating aerosol pH. The sulfate contribution from the fragmentation of common small
691 OS compounds (hydroxymethylsulfonate, methylsulfonic acid) can be distinguished in the AMS using
692 the relative ratio of sulfur containing peaks.(Chen et al., 2019; Javed et al., 2021) However, more
693 work is needed to determine how larger OS and NOS fragment in the AMS such as those quantified
694 in this study. Overall, this highlights that isoprene and MT oxidation can make significant
695 contributions to organic and sulfate-containing aerosol, even in extremely polluted environments
696 such as Delhi. It should be noted that this is just a subset of potentially many more SOA from
697 isoprene and monoterpene markers and only focusses on sulfate containing species.

698

699 **Conclusion**

700 Isoprene- and monoterpene-derived organosulfate (OS) and nitrooxy organosulfate (NOS) species
701 were quantified during pre- and post-monsoon measurement periods in the Indian megacity of
702 Delhi. An extensive dataset of supplementary measurements was obtained alongside filter samples,
703 including isoprene and speciated monoterpenes. Isoprene and monoterpene emissions were found
704 to be highly influenced by anthropogenic sources, with strong correlations to anthropogenic tracers
705 at night across both campaigns. High nocturnal concentrations of pollutants were observed due to a
706 low boundary layer height and stagnant conditions, especially during the post-monsoon period.

707 Isoprene OS markers (OSi) were observed in higher concentrations during the post-monsoon (557 ±
708 423) ng m^{-3} compared to the pre-monsoon campaign (238 ± 118) ng m^{-3}. OSi showed a moderate
709 correlation with inorganic sulfate across both campaigns. However, concentrations levelled off at
710 high sulfate concentrations during the post-monsoon which is consistent with organic coatings
711 limiting uptake of isoprene epoxides. Isoprene NOS species (NOSi) showed nocturnal enhancements
712 across both campaigns, while the highest average concentrations were observed in the morning
713 samples of the post-monsoon campaign. The high morning concentrations are likely due to the
714 oxidation of VOCs by OH radicals from photolytic processes throughout the morning. Monoterpene
715 derived OS (OS$_{MT}$) and NOS (NOS$_{MT}$) markers were observed to have nocturnal enhancements in
716 concentrations, in-line with their precursors. NOS$_{MT}$ markers were observed in similar concentrations
717 to those of other megacities. Total quantified SOA contributed on average (2.0 ± 0.9) % and (1.8 ±
718 1.4) % to the total OOA. Considering high OOA concentrations were observed across the two
719 campaigns, the total markers contributed up to a maximum of 4.2 % and 6.6 % across the pre- and
720 post-monsoon respectively. Overall, this work highlights that even small numbers of isoprene and

721 monoterpene derived SOA markers can make significant contributions to OA mass, even in highly
722 polluted megacities.

723

724 Table 1. Molecular formulae, retention times and time weighted means (ng m^{-3}) of
725 organosulfates (OS) and nitrooxy oganosulfates (NOS) from isoprene (i) and monoterpenes
(MT) observed across pre- and post-monsoon campaigns in Delhi.
726

Class	Molecular formula	Pre-	SD	Post-	SD	RT's (min)
OS$_i$	C$_5$H$_{12}$O$_7$S	38.79	30.19	17.91	19.87	0.71
	C$_5$H$_{10}$O$_5$S	26.16	23.30	53.63	131.19	0.93
	C$_2$H$_4$O$_6$S	21.35	18.27	84.65	82.79	0.73
	C$_5$H$_{10}$O$_6$S	19.80	13.78	45.87	29.47	0.79
	C$_4$H$_8$O$_7$S	19.70	12.48	47.96	39.01	0.73
	C$_3$H$_6$O$_5$S	19.50	12.47	35.27	40.15	0.73
	C$_5$H$_8$O$_7$S	18.76	11.01	38.75	25.34	0.73
	C$_4$H$_8$O$_6$S	16.57	9.77	45.48	37.46	0.74
	C$_5$H$_{10}$O$_7$S	11.82	7.04	25.89	18.06	0.73
	C$_3$H$_6$O$_6$S	6.64	5.00	38.06	40.30	0.73
	C$_4$H$_8$O$_5$S	6.46	4.08	22.44	21.39	0.75
	C$_5$H$_{10}$O$_8$S	6.25	5.07	7.00	5.54	0.73
	C$_2$H$_4$O$_5$S	5.33	3.37	15.92	13.79	0.73
	C$_2$H$_6$O$_5$S	5.23	6.36	24.99	20.38	0.73
	C$_5$H$_8$O$_5$S	5.16	2.57	7.87	7.93	0.85
	C$_3$H$_6$O$_7$S	3.54	3.49	14.78	11.50	0.75
	C$_5$H$_{12}$O$_6$S	2.01	1.23	6.53	4.32	0.74
	C$_3$H$_8$O$_6$S	1.90	1.08	12.25	10.82	0.75
	C$_5$H$_8$O$_9$S	1.20	1.04	2.12	1.85	0.64
	C$_4$H$_6$O$_6$S	1.10	0.76	8.61	15.65	0.74
	C$_5$H$_{12}$O$_8$S	0.55	0.43	0.65	0.61	0.75
	Total	237.83		556.64		
NOS$_i$	C$_5$H$_{10}$O$_{11}$N$_2$S	18.65	8.77	11.63	8.09	1.39,1.92,2.85,3.4
	C$_5$H$_{11}$O$_9$NS	8.55	5.71	5.93	5.06	0.86
	C$_5$H$_9$O$_{10}$NS	3.91	3.46	1.42	1.31	0.94
	C$_5$H$_{11}$O$_8$NS	1.52	0.84	1.17	1.20	1.09
	C$_5$H$_9$O$_{13}$N$_3$S	0.002	0.001	0.011	0.009	6.67,7.89,8.06
	Total	32.63		20.15		
OS$_{MT}$	C$_9$H$_{16}$O$_6$S	1.10	0.61	1.67	0.88	6.67/7.14/7.5/8.3
	C$_{10}$H$_{18}$O$_5$S	0.56	0.63	0.10	0.12	3.39
	C$_{10}$H$_{16}$O$_5$S	0.28	0.13	0.77	0.06	4.91/7/9.08/10.9/11.33/11.97/13.26
	C$_{10}$H$_{20}$O$_7$S	0.25	0.21	0.27	0.21	4.19
	C$_{10}$H$_{16}$O$_7$S	0.23	0.15	0.21	0.13	3.61/11.68
	C$_9$H$_{16}$O$_7$S	0.16	0.17	0.22	0.19	4.39/6.77
	C$_{10}$H$_{18}$O$_6$S	0.15	0.10	NA	NA	10.27

$C_9H_{14}O_6S$	0.15	1.10	0.25	0.14	3.5/5.81
$C_{10}H_{16}O_6S$	0.10	0.06	0.06	0.03	9.33
$C_{10}H_{18}O_8S$	0.02	0.01	0.04	0.24	7.24
$C_8H_{14}O_7S$	0.04	0.03	0.10	0.15	4.46
Total	3.05		3.68		
NOS_{MT} $C_{10}H_{17}NO_7S$	5.96	3.33	13.36	4.98	9.1/10.16/10.67/10.92/11.07/11.36/11.57/12.01/13.28
$C_9H_{15}NO_8S$	1.12	0.51	2.79	1.14	3.5/5.81
$C_{10}H_{17}NO_9S$	0.47	0.19	1.15	0.29	3.93/5.34/6.39/7.89/9.26/10.11/17.94
$C_9H_{15}NO_9S$	0.0216	0.0044	0.22	0.14	2.69/3.46
$C_{10}H_{17}NO_8S$	0.01	0.01	0.07	0.04	5.77
Total	7.59		17.59		

Table 2. Comparison of $C_{10}H_{17}NO_7S$ concentrations across different locations. Locations and concentrations in bold were quantfified by authentic standards.

Location	$C_{10}H_{17}NO_7S$ (ng m^{-3})	Reference
Delhi Pre-monsoon	**5.96**	**This study**
Delhi Post-monsoon	**13.36**	**This study**
Guangzhou summer	7.15	Bryant et al., 2021
Guangzhou winter	11.11	Bryant et al., 2021
Shanghai 15/16	6.21	Wang et al., 2021b
Shanghai 16/17	5.55	Wang et al., 2021b
Beijing	12.00	Wang et al., 2018b
Atlanta	9.00	Hettiyadura et al., 2019
Hong Kong	5.61	Wang et al., 2021a
Guangzhou	12.32	Wang et al., 2021a
Shanghai	16.51	Wang et al., 2021a
Beijing	13.15	Wang et al., 2021a

Data availability

Data used in this study can be accessed from the CEDA archive: https://catalogue.ceda.ac.uk/uuid/ba27c1c6a03b450e9269f668566658ec (Nemitz et al., 2020).

Author contributions

DJB prepared the manuscript with contributions from all authors. DJB, BSN, SJS, SHB, WSD, ARV, JMC, WJFA, BL, EN and JRH provided measurements and data processing of pollutants used in this

study. MJN and ARR contributed to scientific discussion. S, RG, BRG, TH and EN assisted with logistics. CNH, JDL, ARR, JFH provided overall guidance to the experimental setup and design.

Acknowledgements

The authors acknowledge Tuhin Mandal at CSIR-National Physical Laboratory for his support in facilitating the measurement sites used in this project and Gareth Stewart for the VOC measurements. This work was supported by the Newton Bhabha fund administered by the UK Natural Environment Research Council through the DelhiFlux and ASAP projects of the Atmospheric Pollution and Human Health in an Indian Megacity (APHH-India) programme. The authors gratefully acknowledge the financial support provided by the UK Natural Environment Research Council and the Earth System Science Organization, Ministry of Earth Sciences, Government of India, under the Indo-UK Joint Collaboration (DelhiFlux). Daniel J. Bryant and Beth S. Nelson acknowledge the NERC SPHERES doctoral training programme for studentships. James M. Cash is supported by a NERC E3 DTP studentship.

Financial support

This research has been supported by the Natural Environment Research Council (grant nos. NE/P016502/1 and NE/P01643X/1) and the Govt. of India, Ministry of Earth Sciences (grant no. MoES/16/19/2017/APHH, DelhiFlux).

Competing interests

The authors declare that they have no conflict of interest.

References

Anand, V., Korhale, N., Rathod, A. and Beig, G.: On processes controlling fine particulate matters in four Indian megacities, Environ. Pollut., 254, doi:10.1016/j.envpol.2019.113026, 2019.

Anon: Import Surface Meteorological Data from NOAA Integrated Surface Database (ISD) • worldmet, [online] Available from: https://davidcarslaw.github.io/worldmet/index.html (Accessed 24 October 2021), n.d.

Åsa M. Jonsson, *, Mattias Hallquist, and and Ljungström, E.: Impact of Humidity on the Ozone Initiated Oxidation of Limonene, Δ3-Carene, and α-Pinene, Environ. Sci. Technol., 40(1), 188–194, doi:10.1021/ES051163W, 2005.

Atkinson, R. and Arey, J.: Gas-phase tropospheric chemistry of biogenic volatile organic compounds: A review, Atmos. Environ., 37(SUPPL. 2), 197–219, doi:10.1016/S1352-2310(03)00391-1, 2003.

Balakrishnan, K., Dey, S., Gupta, T., Dhaliwal, R. S., Brauer, M., Cohen, A. J., Stanaway, J. D., Beig, G., Joshi, T. K., Aggarwal, A. N., Sabde, Y., Sadhu, H., Frostad, J., Causey, K., Godwin, W., Shukla, D. K., Kumar, G. A., Varghese, C. M., Muraleedharan, P., Agrawal, A., Anjana, R. M., Bhansali, A., Bhardwaj, D., Burkart, K., Cercy, K., Chakma, J. K., Chowdhury, S., Christopher, D. J., Dutta, E., Furtado, M., Ghosh, S., Ghoshal, A. G., Glenn, S. D., Guleria, R., Gupta, R., Jeemon, P., Kant, R., Kant, S., Kaur, T., Koul, P. A., Krish, V., Krishna, B., Larson, S. L., Madhipatla, K., Mahesh, P. A., Mohan, V., Mukhopadhyay, S., Mutreja, P., Naik, N., Nair, S., Nguyen, G., Odell, C. M., Pandian, J. D., Prabhakaran, D., Prabhakaran, P., Roy, A., Salvi, S., Sambandam, S., Saraf, D., Sharma, M., Shrivastava, A., Singh, V., Tandon, N., Thomas, N. J., Torre, A., Xavier, D., Yadav, G., Singh, S., Shekhar, C., Vos, T., Dandona, R., Reddy, K. S., Lim, S. S., Murray, C. J. L., Venkatesh, S. and Dandona, L.: The impact of air pollution on deaths, disease burden, and life expectancy across the states of India: the Global Burden of Disease Study 2017, Lancet Planet. Heal., 3(1), e26–e39, doi:10.1016/S2542-5196(18)30261-4, 2019.

Bhandari, S., Gani, S., Patel, K., Wang, D. S., Soni, P., Arub, Z., Habib, G., Apte, J. S. and Hildebrandt Ruiz, L.: Sources and atmospheric dynamics of organic aerosol in New Delhi, India: Insights from receptor modeling, Atmos. Chem. Phys., 20(2), 735–752, doi:10.5194/acp-20-735-2020, 2020.

Borbon, A., Fontaine, H., Veillerot, M., Locoge, N., Galloo, J. C. and Guillermo, R.: An investigation into the traffic-related fraction of isoprene at an urban location, Atmos. Environ., 35(22), 3749–3760, doi:10.1016/S1352-2310(01)00170-4, 2001.

Brüggemann, M., van Pinxteren, D., Wang, Y., Yu, J. Z. and Herrmann, H.: Quantification of known and unknown terpenoid organosulfates in PM10 using untargeted LC–HRMS/MS: contrasting summertime rural Germany and the North China Plain, Environ. Chem., 16(5), 333, doi:10.1071/EN19089, 2019.

Brüggemann, M., Xu, R., Tilgner, A., Kwong, K. C., Mutzel, A., Poon, H. Y., Otto, T., Schaefer, T., Poulain, L., Chan, M. N. and Herrmann, H.: Organosulfates in Ambient Aerosol: State of Knowledge and Future Research Directions on Formation, Abundance, Fate, and Importance, Environ. Sci. Technol., 54(7), 3767–3782, doi:10.1021/acs.est.9b06751, 2020a.

Brüggemann, M., Riva, M., Perrier, S., Poulain, L., George, C. and Herrmann, H.: Overestimation of Monoterpene Organosulfate Abundance in Aerosol Particles by Sampling in the Presence of SO2, Environ. Sci. Technol. Lett., 8, 206–211, doi:10.1021/acs.estlett.0c00814, 2020b.

Bryant, D. J., Dixon, W. J., Hopkins, J. R., Dunmore, R. E., Pereira, K. L., Shaw, M., Squires, F. A., Bannan, T. J., Mehra, A., Worrall, S. D., Bacak, A., Coe, H., Percival, C. J., Whalley, L. K., Heard, D. E., Slater, E. J., Ouyang, B., Cui, T., Surratt, J. D., Liu, D., Shi, Z., Harrison, R., Sun, Y., Xu, W., Lewis, A. C., Lee, J. D., Rickard, A. R. and Hamilton, J. F.: Strong anthropogenic control of secondary organic aerosol formation from isoprene in Beijing, Atmos. Chem. Phys., 20(12), 7531–7552, doi:10.5194/acp-20-7531-2020, 2020.

Bryant, D. J., Elzein, A., Newland, M., White, E., Swift, S., Watkins, A., Deng, W., Song, W., Wang, S., Zhang, Y., Wang, X., Rickard, A. R. and Hamilton, J. F.: Importance of Oxidants and Temperature in the Formation of Biogenic Organosulfates and Nitrooxy Organosulfates, ACS Earth Sp. Chem., acsearthspacechem.1c00204, doi:10.1021/ACSEARTHSPACECHEM.1C00204, 2021.

Budisulistiorini, S. H., Li, X., Bairai, S. T., Renfro, J., Liu, Y., Liu, Y. J., McKinney, K. A., Martin, S. T., McNeill, V. F., Pye, H. O. T., Nenes, A., Neff, M. E., Stone, E. A., Mueller, S., Knote, C., Shaw, S. L., Zhang, Z., Gold, A. and Surratt, J. D.: Examining the effects of anthropogenic emissions on isoprene-derived secondary organic aerosol formation during the 2013 Southern Oxidant and Aerosol Study (SOAS) at the Look Rock, Tennessee ground site, Atmos. Chem. Phys., 15(15), 8871–8888, doi:10.5194/acp-15-8871-2015, 2015.

Cash, J. M., Langford, B., Di Marco, C., Mullinger, N. J., Allan, J., Reyes-Villegas, E., Joshi, R., Heal, M. R., Acton, W. J. F., Hewitt, C. N., Misztal, P. K., Drysdale, W., Mandal, T. K., Gadi, R., Gurjar, B. R. and Nemitz, E.: Seasonal analysis of submicron aerosol in Old Delhi using high-resolution aerosol mass spectrometry: chemical characterisation, source apportionment and new marker identification, Atmos. Chem. Phys., 21(13), 10133–10158, doi:10.5194/ACP-21-10133-2021, 2021a.

Cash, J. M., Langford, B., Di Marco, C., Mullinger, N. J., Allan, J., Reyes-Villegas, E., Joshi, R., Heal, M. R., Acton, W. J. F., Hewitt, C. N., Misztal, P. K., Drysdale, W., Mandal, T. K., Shivani, Gadi, R., Gurjar, B. R. and Nemitz, E.: Seasonal analysis of submicron aerosol in Old Delhi using high-resolution aerosol mass spectrometry: Chemical characterisation, source apportionment and new marker identification, Atmos. Chem. Phys., 21(13), 10133–10158, doi:10.5194/ACP-21-10133-2021, 2021b.

Chan, M. N., Surratt, J. D., Chan, A. W. H., Schilling, K., Offenberg, J. H., Lewandowski, M., Edney, E. O., Kleindienst, T. E., Jaoui, M., Edgerton, E. S., Tanner, R. L., Shaw, S. L., Zheng, M., Knipping, E. M. and Seinfeld, J. H.: Influence of aerosol acidity on the chemical composition of Secondary Organic

Aerosol from β-caryophyllene, Atmos. Chem. Phys. Discuss., 10(11), 29249–29289, doi:10.5194/acpd-10-29249-2010, 2010.

Chen, Y., Xu, L., Humphry, T., Hettiyadura, A. P. S., Ovadnevaite, J., Huang, S., Poulain, L., Schroder, J. C., Campuzano-Jost, P., Jimenez, J. L., Herrmann, H., O'Dowd, C., Stone, E. A. and Ng, N. L.: Response of the Aerodyne Aerosol Mass Spectrometer to Inorganic Sulfates and Organosulfur Compounds: Applications in Field and Laboratory Measurements, Environ. Sci. Technol., 53(9), 5176–5186, doi:10.1021/ACS.EST.9B00884/ASSET/IMAGES/MEDIUM/ES-2019-00884R_0003.GIF, 2019.

Chen, Y., Zhang, Y., T. Lambe, A., Xu, R., Lei, Z., E. Olson, N., Zhang, Z., Szalkowski, T., Cui, T., Vizuete, W., Gold, A., J. Turpin, B., P Ault, A., Nin Chan, M. and D. Surratt, J.: Heterogeneous Hydroxyl Radical Oxidation of Isoprene Epoxydiol-Derived Methyltetrol Sulfates: Plausible Formation Mechanisms of Previously Unexplained Organosulfates in Ambient Fine Aerosols, Environ. Sci. & Technol. Lett., 0(ja), doi:10.1021/acs.estlett.0c00276, 2020.

Cheng, X., Li, H., Zhang, Y., Li, Y., Zhang, W., Wang, X., Bi, F., Zhang, H., Gao, J., Chai, F., Lun, X., Chen, Y. and Lv, J.: Atmospheric isoprene and monoterpenes in a typical urban area of Beijing: Pollution characterization, chemical reactivity and source identification, J. Environ. Sci., 71, 150–167, doi:10.1016/J.JES.2017.12.017, 2018.

Chowdhury, Z., Zheng, M., Cass, G. R., Sheesley, R. J., Schauer, J. J., Salmon, L. G. and Russell, A. G.: Source apportionment and characterization of ambient fine particles in Delhi, in Symposium on Air Quality Measurement Methods and Technology 2004, pp. 13–24., 2004.

Coggona, M. M., Gkatzelis, G. I., McDonald, B. C., Gilman, J. B., Schwantes, R. H., Abuhassan, N., Aikin, K. C., Arendd, M. F., Berkoff, T. A., Brown, S. S., Campos, T. L., Dickerson, R. R., Gronoff, G., Hurley, J. F., Isaacman-Vanwertz, G., Koss, A. R., Li, M., McKeen, S. A., Moshary, F., Peischl, J., Pospisilova, V., Ren, X., Wilson, A., Wu, Y., Trainer, M. and Warneke, C.: Volatile chemical product emissions enhance ozone and modulate urban chemistry, Proc. Natl. Acad. Sci. U. S. A., 118(32), e2026653118, doi:10.1073/PNAS.2026653118/SUPPL_FILE/PNAS.2026653118.SAPP.PDF, 2021.

Darer, A. I., Cole-Filipiak, N. C., O'Connor, A. E. and Elrod, M. J.: Formation and stability of atmospherically relevant isoprene-derived organosulfates and organonitrates, Environ. Sci. Technol., 45(5), 1895–1902, doi:10.1021/es103797z, 2011.

Ding, J., Zhao, P., Su, J., Dong, Q., Du, X. and Zhang, Y.: Aerosol pH and its driving factors in Beijing, Atmos. Chem. Phys., 19(12), 7939–7954, doi:10.5194/ACP-19-7939-2019, 2019.

Drozd, G. T., Woo, J. L. and McNeill, V. F.: Self-limited uptake of α-pinene oxide to acidic aerosol: The effects of liquid-liquid phase separation and implications for the formation of secondary organic aerosol and organosulfates from epoxides, Atmos. Chem. Phys., 13(16), 8255–8263, doi:10.5194/acp-13-8255-2013, 2013.

Du, Z., He, K., Cheng, Y., Duan, F., Ma, Y., Liu, J., Zhang, X., Zheng, M. and Weber, R.: A yearlong study of water-soluble organic carbon in Beijing I: Sources and its primary vs. secondary nature, Atmos. Environ., 92, 514–521, doi:10.1016/j.atmosenv.2014.04.060, 2014.

Eddingsaas, N. C., Loza, C. L., Yee, L. D., Seinfeld, J. H. and Wennberg, P. O.: α-pinene photooxidation under controlled chemical conditions-Part 1: Gas-phase composition in low-and high-NO xenvironments, Atmos. Chem. Phys., 12(14), 6489–6504, doi:10.5194/acp-12-6489-2012, 2012a.

Eddingsaas, N. C., Loza, C. L., Yee, L. D., Chan, M., Schilling, K. A., Chhabra, P. S., Seinfeld, J. H. and Wennberg, P. O.: α-pinene photooxidation under controlled chemical conditions-Part 2: SOA yield and composition in low-and high-NO x environments, Atmos. Chem. Phys., 12(16), 7413–7427, doi:10.5194/acp-12-7413-2012, 2012b.

875 Elser, M., Huang, R. J., Wolf, R., Slowik, J. G., Wang, Q., Canonaco, F., Li, G., Bozzetti, C., Daellenbach,
876 K. R., Huang, Y., Zhang, R., Li, Z., Cao, J., Baltensperger, U., El-Haddad, I. and André, P.: New insights
877 into PM2.5 chemical composition and sources in two major cities in China during extreme haze
878 events using aerosol mass spectrometry, Atmos. Chem. Phys., 16(5), 3207–3225, doi:10.5194/ACP-
879 16-3207-2016, 2016.

880 Elzein, A., Stewart, G. J., Swift, S. J., Nelson, B. S., Crilley, L. R., Alam, M. S., Reyes-Villegas, E., Gadi,
881 R., Harrison, R. M., Hamilton, J. F. and Lewis, A. C.: A comparison of PM2.5-bound polycyclic
882 aromatic hydrocarbons in summer Beijing (China) and Delhi (India), Atmos. Chem. Phys., 20(22),
883 14303–14319, doi:10.5194/ACP-20-14303-2020, 2020.

884 Galloway, M. M., Chhabra, P. S., Chan, A. W. H., Surratt, J. D., Flagan, R. C., Seinfeld, J. H. and
885 Keutsch, F. N.: Glyoxal uptake on ammonium sulphate seed aerosol: Reaction products and
886 reversibility of uptake under dark and irradiated conditions, Atmos. Chem. Phys., 9(10), 3331–3345,
887 doi:10.5194/acp-9-3331-2009, 2009.

888 Gani, S., Bhandari, S., Seraj, S., Wang, D. S., Patel, K., Soni, P., Arub, Z., Habib, G., Hildebrandt Ruiz, L.
889 and Apte, J. S.: Submicron aerosol composition in the world's most polluted megacity: the Delhi
890 Aerosol Supersite study, Atmos. Chem. Phys., 19(10), 6843–6859, doi:10.5194/acp-19-6843-2019,
891 2019.

892 Gaston, C. J., Riedel, T. P., Zhang, Z., Gold, A., Surratt, J. D. and Thornton, J. A.: Reactive Uptake of an
893 Isoprene-Derived Epoxydiol to Submicron Aerosol Particles, Environ. Sci. Technol., 48(19), 11178–
894 11186, doi:10.1021/es5034266, 2014.

895 Gkatzelis, G. I., Coggon, M. M., McDonald, B. C., Peischl, J., Gilman, J. B., Aikin, K. C., Robinson, M. A.,
896 Canonaco, F., Prevot, A. S. H., Trainer, M. and Warneke, C.: Observations Confirm that Volatile
897 Chemical Products Are a Major Source of Petrochemical Emissions in U.S. Cities, Environ. Sci.
898 Technol., 55(8), 4332–4343, doi:10.1021/ACS.EST.0C05471/SUPPL_FILE/ES0C05471_SI_001.PDF,
899 2021.

900 Glasius, M., Bering, M. S., Yee, L. D., de Sá, S. S., Isaacman-VanWertz, G., Wernis, R. A., Barbosa, H.
901 M. J., Alexander, M. L., Palm, B. B., Hu, W., Campuzano-Jost, P., Day, D. A., Jimenez, J. L., Shrivastava,
902 M., Martin, S. T. and Goldstein, A. H.: Organosulfates in aerosols downwind of an urban region in
903 central Amazon, Environ. Sci. Process. Impacts, 20(11), 1546–1558, doi:10.1039/C8EM00413G, 2018.

904 Guenther, A. B., Jiang, X., Heald, C. L., Sakulyanontvittaya, T., Duhl, T., Emmons, L. K. and Wang, X.:
905 The Model of Emissions of Gases and Aerosols from Nature version 2.1 (MEGAN2.1): an extended
906 and updated framework for modeling biogenic emissions, Geosci. Model Dev., 5(6), 1471–1492,
907 doi:10.5194/gmd-5-1471-2012, 2012.

908 Hallquist, M., Wenger, J. C., Baltensperger, U., Rudich, Y., Simpson, D., Claeys, M., Dommen, J.,
909 Donahue, N. M., George, C., Goldstein, A. H., Hamilton, J. F., Herrmann, H., Hoffmann, T., Iinuma, Y.,
910 Jang, M., Jenkin, M. E., Jimenez, J. L., Kiendler-Scharr, A., Maenhaut, W., McFiggans, G., Mentel, T. F.,
911 Monod, A., Prévôt, A. S. H., Seinfeld, J. H., Surratt, J. D., Szmigielski, R. and Wildt, J.: The formation,
912 properties and impact of secondary organic aerosol: current and emerging issues, Atmos. Chem.
913 Phys., 9(14), 5155–5236, doi:10.5194/acp-9-5155-2009, 2009.

914 Hama, S. M. L., Kumar, P., Harrison, R. M., Bloss, W. J., Khare, M., Mishra, S., Namdeo, A., Sokhi, R.,
915 Goodman, P. and Sharma, C.: Four-year assessment of ambient particulate matter and trace gases in
916 the Delhi-NCR region of India, Sustain. Cities Soc., 54, doi:10.1016/j.scs.2019.102003, 2020.

917 Hamilton, J. F., Bryant, D. J., Edwards, P. M., Ouyang, B., Bannan, T. J., Mehra, A., Mayhew, A. W.,
918 Hopkins, J. R., Dunmore, R. E., Squires, F. A., Lee, J. D., Newland, M. J., Worrall, S. D., Bacak, A., Coe,
919 H., Whalley, L. K., Heard, D. E., Slater, E. J., Jones, R. L., Cui, T., Surratt, J. D., Reeves, C. E., Mills, G. P.,
920 Grimmond, S., Sun, Y., Xu, W., Shi, Z. and Rickard, A. R.: Key Role of NO3 Radicals in the Production

921   of Isoprene Nitrates and Nitrooxyorganosulfates in Beijing, Environ. Sci. Technol., 55(2), 842–853,
922   doi:10.1021/acs.est.0c05689, 2021.

923   Hatch, L. E., Jen, C. N., Kreisberg, N. M., Selimovic, V., Yokelson, R. J., Stamatis, C., York, R. A., Foster,
924   D., Stephens, S. L., Goldstein, A. H. and Barsanti, K. C.: Highly Speciated Measurements of Terpenoids
925   Emitted from Laboratory and Mixed-Conifer Forest Prescribed Fires, Environ. Sci. Technol., 53(16),
926   9418–9428, doi:10.1021/ACS.EST.9B02612, 2019.

927   Hettiyadura, A. P. S., Al-Naiema, I. M., Hughes, D. D., Fang, T. and Stone, E. A.: Organosulfates in
928   Atlanta, Georgia: anthropogenic influences on biogenic secondary organic aerosol formation, Atmos.
929   Chem. Phys., 19(5), 3191–3206, doi:10.5194/acp-19-3191-2019, 2019.

930   Hoffmann, T., Odum, J. R., Bowman, F., Collins, D., Klockow, D., Flagan, R. C. and Seinfeld, J. H.:
931   Formation of organic aerosols from the oxidation of biogenic hydrocarbons, J. Atmos. Chem., 26(2),
932   189–222, doi:10.1023/A:1005734301837, 1997.

933   Hoyle, C. R., Boy, M., Donahue, N. M., Fry, J. L., Glasius, M., Guenther, A., Hallar, A. G., Huff Hartz, K.,
934   Petters, M. D., Petäjä, T., Rosenoern, T. and Sullivan, A. P.: A review of the anthropogenic influence
935   on biogenic secondary organic aerosol, Atmos. Chem. Phys., 11(1), 321–343, doi:10.5194/acp-11-
936   321-2011, 2011.

937   Hsieh, H.-C., Ou-Yang, C.-F. and Wang, J.-L.: Revelation of Coupling Biogenic with Anthropogenic
938   Isoprene by Highly Time-Resolved Observations, Aerosol Air Qual. Res., 17(3), 721–729,
939   doi:10.4209/AAQR.2016.04.0133, 2017.

940   Hu, W., Hu, M., Hu, W., Jimenez, J. L., Yuan, B., Chen, W., Wang, M., Wu, Y., Chen, C., Wang, Z., Peng,
941   J., Zeng, L. and Shao, M.: Chemical composition, sources, and aging process of submicron aerosols in
942   Beijing: Contrast between summer and winter, J. Geophys. Res. Atmos., 121(4), 1955–1977,
943   doi:10.1002/2015JD024020, 2016.

944   Huang, Z., Zhang, Y., Yan, Q., Zhang, Z. and Wang, X.: Real-time monitoring of respiratory absorption
945   factors of volatile organic compounds in ambient air by proton transfer reaction time-of-flight mass
946   spectrometry, J. Hazard. Mater., 320, 547–555, doi:10.1016/J.JHAZMAT.2016.08.064, 2016.

947   Iinuma, Y., Müller, C., Berndt, T., Böge, O., Claeys, M. and Herrmann, H.: Evidence for the existence
948   of organosulfates from β-pinene ozonolysis in ambient secondary organic aerosol, Environ. Sci.
949   Technol., 41(19), 6678–6683, doi:10.1021/es070938t, 2007.

950   Jain, N., Bhatia, A. and Pathak, H.: Emission of Air Pollutants from Crop Residue Burning in India,
951   Aerosol Air Qual. Res., 14(1), 422–430, doi:10.4209/aaqr.2013.01.0031, 2014.

952   Javed, M., Bashir, M. and Zaineb, S.: Analysis of daily and seasonal variation of fine particulate
953   matter (PM2.5) for five cities of China, Environ. Dev. Sustain., 1–29, doi:10.1007/s10668-020-01159-
954   1, 2021.

955   Kanawade, V. P., Srivastava, A. K., Ram, K., Asmi, E., Vakkari, V., Soni, V. K., Varaprasad, V. and
956   Sarangi, C.: What caused severe air pollution episode of November 2016 in New Delhi?, Atmos.
957   Environ., 222, doi:10.1016/j.atmosenv.2019.117125, 2020.

958   Kashyap, P., Kumar, A., Kumar, R. P. and Kumar, K.: Biogenic and anthropogenic isoprene emissions
959   in the subtropical urban atmosphere of Delhi, Atmos. Pollut. Res., 10(5), 1691–1698,
960   doi:10.1016/j.apr.2019.07.004, 2019.

961   Khan, M. A. H., Schlich, B.-L., Jenkin, M. E., Shallcross, B. M. A., Moseley, K., Walker, C., Morris, W. C.,
962   Derwent, R. G., Percival, C. J. and Shallcross, D. E.: A Two-Decade Anthropogenic and Biogenic
963   Isoprene Emissions Study in a London Urban Background and a London Urban Traffic Site, Atmos.
964   2018, Vol. 9, Page 387, 9(10), 387, doi:10.3390/ATMOS9100387, 2018a.

Khan, M. A. H., Schlich, B. L., Jenkin, M. E., Shallcross, B. M. A., Moseley, K., Walker, C., Morris, W. C., Derwent, R. G., Percival, C. J. and Shallcross, D. E.: A Two-Decade Anthropogenic and Biogenic Isoprene Emissions Study in a London Urban Background and a London Urban Traffic Site, Atmos. 2018, Vol. 9, Page 387, 9(10), 387, doi:10.3390/ATMOS9100387, 2018b.

Kirillova, E. N., Sheesley, R. J., Andersson, A. and Gustafsson, Ö.: Natural abundance 13C and 14C analysis of water-soluble organic carbon in atmospheric aerosols, Anal. Chem., 82(19), 7973–7978, doi:10.1021/ac1014436, 2010.

Kirillova, E. N., Andersson, A., Sheesley, R. J., Kruså, M., Praveen, P. S., Budhavant, K., Safai, P. D., Rao, P. S. P. and Gustafsson, Ö.: ^{13}C- and ^{14}C-based study of sources and atmospheric processing of water-soluble organic carbon (WSOC) in South Asian aerosols, J. Geophys. Res. Atmos., 118(2), 614–626, doi:10.1002/jgrd.50130, 2013.

Kirillova, E. N., Andersson, A., Tiwari, S., Srivastava, A. K., Bisht, D. S. and Gustafsson, Ö.: Water-soluble organic carbon aerosols during a full New Delhi winter: Isotope-based source apportionment and optical properties, J. Geophys. Res. Atmos., 119(6), 3476–3485, doi:10.1002/2013JD020041, 2014.

Klein, F., Farren, N. J., Bozzetti, C., Daellenbach, K. R., Kilic, D., Kumar, N. K., Pieber, S. M., Slowik, J. G., Tuthill, R. N., Hamilton, J. F., Baltensperger, U., Prévôt, A. S. H. and El Haddad, I.: Indoor terpene emissions from cooking with herbs and pepper and their secondary organic aerosol production potential, Sci. Reports 2016 61, 6(1), 1–7, doi:10.1038/srep36623, 2016.

Kleindienst, T. E., Edney, E. O., Lewandowski, M., Offenberg, J. H. and Jaoui, M.: Secondary Organic Carbon and Aerosol Yields from the Irradiations of Isoprene and α-Pinene in the Presence of NO$_x$ and SO$_2$, Environ. Sci. Technol., 40(12), 3807–3812, doi:10.1021/es052446r, 2006.

Kourtchev, I., Godoi, R. H. M., Connors, S., Levine, J. G., Archibald, A. T., Godoi, A. F. L., Paralovo, S. L., Barbosa, C. G. G., Souza, R. A. F., Manzi, A. O., Seco, R., Sjostedt, S., Park, J. H., Guenther, A., Kim, S., Smith, J., Martin, S. T. and Kalberer, M.: Molecular composition of organic aerosols in central Amazonia: An ultra-high-resolution mass spectrometry study, Atmos. Chem. Phys., 16(18), 11899–11913, doi:10.5194/acp-16-11899-2016, 2016.

Kristensen, K., Enggrob, K. L., King, S. M., Worton, D. R., Platt, S. M., Mortensen, R., Rosenoern, T., Surratt, J. D., Bilde, M., Goldstein, A. H. and Glasius, M.: Formation and occurrence of dimer esters of pinene oxidation products in atmospheric aerosols, Atmos. Chem. Phys., 13(7), 3763–3776, doi:10.5194/acp-13-3763-2013, 2013.

Kumar, P., Kumar, S. and Yadav, S.: Seasonal variations in size distribution, water-soluble ions, and carbon content of size-segregated aerosols over New Delhi, Environ. Sci. Pollut. Res., 25(6), 6061–6078, doi:10.1007/S11356-017-0954-6, 2018.

Landrigan, P. J., Fuller, R., Acosta, N. J. R., Adeyi, O., Arnold, R., Basu, N. (Nil), Baldé, A. B., Bertollini, R., Bose-O'Reilly, S., Boufford, J. I., Breysse, P. N., Chiles, T., Mahidol, C., Coll-Seck, A. M., Cropper, M. L., Fobil, J., Fuster, V., Greenstone, M., Haines, A., Hanrahan, D., Hunter, D., Khare, M., Krupnick, A., Lanphear, B., Lohani, B., Martin, K., Mathiasen, K. V, McTeer, M. A., Murray, C. J. L., Ndahimananjara, J. D., Perera, F., Potočnik, J., Preker, A. S., Ramesh, J., Rockström, J., Salinas, C., Samson, L. D., Sandilya, K., Sly, P. D., Smith, K. R., Steiner, A., Stewart, R. B., Suk, W. A., van Schayck, O. C. P., Yadama, G. N., Yumkella, K. and Zhong, M.: The Lancet Commission on pollution and health, Lancet, 391(10119), 462–512, doi:10.1016/S0140-6736(17)32345-0, 2018.

Lanz, V. A., Pŕev̂ot, A. S. H., Alfarra, M. R., Weimer, S., Mohr, C., Decarlo, P. F., Gianini, M. F. D., Hueglin, C., Schneider, J., Favez, O., D'Anna, B., George, C. and Baltensperger, U.: Characterization of aerosol chemical composition with aerosol mass spectrometry in Central Europe: An overview, Atmos. Chem. Phys., 10(21), 10453–10471, doi:10.5194/ACP-10-10453-2010, 2010.

1011 Lee, B. H., Mohr, C., Lopez-Hilfiker, F. D., Lutz, A., Hallquist, M., Lee, L., Romer, P., Cohen, R. C., Iyer,
1012 S., Kurtén, T., Hu, W., Day, D. A., Campuzano-Jost, P., Jimenez, J. L., Xu, L., Ng, N. L., Guo, H., Weber,
1013 R. J., Wild, R. J., Brown, S. S., Koss, A., de Gouw, J., Olson, K., Goldstein, A. H., Seco, R., Kim, S.,
1014 McAvey, K., Shepson, P. B., Starn, T., Baumann, K., Edgerton, E. S., Liu, J., Shilling, J. E., Miller, D. O.,
1015 Brune, W., Schobesberger, S., D'Ambro, E. L. and Thornton, J. A.: Highly functionalized organic
1016 nitrates in the southeast United States: Contribution to secondary organic aerosol and reactive
1017 nitrogen budgets., Proc. Natl. Acad. Sci. U. S. A., 113(6), 1516–21, doi:10.1073/pnas.1508108113,
1018 2016.

1019 Lelieveld, J., Gromov, S., Pozzer, A. and Taraborrelli, D.: Global tropospheric hydroxyl distribution,
1020 budget and reactivity, Atmos. Chem. Phys., 16(19), 12477–12493, doi:10.5194/ACP-16-12477-2016,
1021 2016.

1022 Liao, J., Froyd, K. D., Murphy, D. M., Keutsch, F. N., Yu, G., Wennberg, P. O., St. Clair, J. M., Crounse,
1023 J. D., Wisthaler, A., Mikoviny, T., Jimenez, J. L., Campuzano-Jost, P., Day, D. A., Hu, W., Ryerson, T. B.,
1024 Pollack, I. B., Peischl, J., Anderson, B. E., Ziemba, L. D., Blake, D. R., Meinardi, S. and Diskin, G.:
1025 Airborne measurements of organosulfates over the continental U.S., J. Geophys. Res., 120(7), 2990–
1026 3005, doi:10.1002/2014JD022378, 2015.

1027 Lin, Y. H., Zhang, Z., Docherty, K. S., Zhang, H., Budisulistiorini, S. H., Rubitschun, C. L., Shaw, S. L.,
1028 Knipping, E. M., Edgerton, E. S., Kleindienst, T. E., Gold, A. and Surratt, J. D.: Isoprene epoxydiols as
1029 precursors to secondary organic aerosol formation: Acid-catalyzed reactive uptake studies with
1030 authentic compounds, Environ. Sci. Technol., 46(1), 250–258, doi:10.1021/es202554c, 2012.

1031 Lin, Y. H., Zhang, H., Pye, H. O. T., Zhang, Z., Marth, W. J., Park, S., Arashiro, M., Cui, T.,
1032 Budisulistiorini, S. H., Sexton, K. G., Vizuete, W., Xie, Y., Luecken, D. J., Piletic, I. R., Edney, E. O.,
1033 Bartolotti, L. J., Gold, A. and Surratt, J. D.: Epoxide as a precursor to secondary organic aerosol
1034 formation from isoprene photooxidation in the presence of nitrogen oxides, Proc. Natl. Acad. Sci. U.
1035 S. A., 110(17), 6718–6723, doi:10.1073/pnas.1221150110, 2013a.

1036 Lin, Y. H., Knipping, E. M., Edgerton, E. S., Shaw, S. L. and Surratt, J. D.: Investigating the influences of
1037 SO2 and NH3 levels on isoprene-derived secondary organic aerosol formation using conditional
1038 sampling approaches, Atmos. Chem. Phys., 13(16), 8457–8470, doi:10.5194/ACP-13-8457-2013,
1039 2013b.

1040 Lin, Y. H., Budisulistiorini, S. H., Chu, K., Siejack, R. A., Zhang, H., Riva, M., Zhang, Z., Gold, A.,
1041 Kautzman, K. E. and Surratt, J. D.: Light-absorbing oligomer formation in secondary organic aerosol
1042 from reactive uptake of isoprene epoxydiols, Environ. Sci. Technol., 48(20), 12012–12021,
1043 doi:10.1021/es503142b, 2014.

1044 Mishra, A. K. and Sinha, V.: Emission drivers and variability of ambient isoprene, formaldehyde and
1045 acetaldehyde in north-west India during monsoon season, Environ. Pollut., 267, 115538,
1046 doi:10.1016/J.ENVPOL.2020.115538, 2020.

1047 Miyazaki, Y., Aggarwal, S. G., Singh, K., Gupta, P. K. and Kawamura, K.: Dicarboxylic acids and water-
1048 soluble organic carbon in aerosols in New Delhi, India, in winter: Characteristics and formation
1049 processes, J. Geophys. Res. Atmos., 114(19), doi:10.1029/2009JD011790, 2009.

1050 Morales, A. C., Jayarathne, T., Slade, J. H., Laskin, A. and Shepson, P. B.: The production and
1051 hydrolysis of organic nitrates from OH radical oxidation of β-ocimene, Atmos. Chem. Phys., 21(1),
1052 129–145, doi:10.5194/ACP-21-129-2021, 2021.

1053 Mutzel, A., Rodigast, M., Iinuma, Y., Böge, O. and Herrmann, H.: Monoterpene SOA - Contribution of
1054 first-generation oxidation products to formation and chemical composition, Atmos. Environ., 130,
1055 136–144, doi:10.1016/j.atmosenv.2015.10.080, 2016.

Nagar, P. K., Singh, D., Sharma, M., Kumar, A., Aneja, V. P., George, M. P., Agarwal, N. and Shukla, S. P.: Characterization of PM2.5 in Delhi: role and impact of secondary aerosol, burning of biomass, and municipal solid waste and crustal matter, Environ. Sci. Pollut. Res., 24(32), 25179–25189, doi:10.1007/s11356-017-0171-3, 2017.

Nelson, B., Stewart, G., Drysdale, W., Newland, M., Vaughan, A., Dunmore, R., Edwards, P., Lewis, A., Hamilton, J., Acton, W. J. F., Hewitt, C. N., Crilley, L., Alam, M., Şahin, Ü., Beddows, D., Bloss, W., Slater, E., Whalley, L., Heard, D., Cash, J., Langford, B., Nemitz, E., Sommariva, R., Cox, S., Gadi, R., Gurjar, B., Hopkins, J., Rickard, A. and Lee, J.: In situ Ozone Production is highly sensitive to Volatile Organic Compounds in the Indian Megacity of Delhi, Atmos. Chem. Phys. Discuss., 1–36, doi:10.5194/ACP-2021-278, 2021.

Nestorowicz, K., Jaoui, M., Rudzinski, K. J., Lewandowski, M., Kleindienst, T. E., Spólnik, G., Danikiewicz, W. and Szmigielski, R.: Chemical composition of isoprene SOA under acidic and non-acidic conditions: effect of relative humidity, Atmos. Chem. Phys., 18(24), 18101–18121, doi:10.5194/acp-18-18101-2018, 2018.

Newland, M. J., Bryant, D. J., Dunmore, R. E., Bannan, T. J., Joe, W., Langford, B., Hopkins, J. R., Squires, F. A., Dixon, W., Drysdale, W. S., Ivatt, P. D., Evans, M. J., Edwards, P. M., Whalley, L. K., Heard, D. E., Slater, E. J., Woodward-Massey, R., Ye, C., Mehra, A., Worrall, S. D., Bacak, A., Coe, H., Percival, C. J., Nicholas Hewitt, C., Lee, J. D., Cui, T., Surratt, J. D., Wang, X., Lewis, A. C., Rickard, A. R. and Hamilton, J. F.: Low-NO atmospheric oxidation pathways in a polluted megacity, Atmos. Chem. Phys., 21(3), 1613–1625, doi:10.5194/acp-21-1613-2021, 2021.

Ng, N. L., Kwan, A. J., Surratt, J. D., Chan, A. W. H., Chhabra, P. S., Sorooshian, A., Pye, H. O. T., Crounse, J. D., Wennberg, P. O., Flagan, R. C. and Seinfeld, J. H.: Secondary organic aerosol (SOA) formation from reaction of isoprene with nitrate radicals (NO3), Atmos. Chem. Phys., 8(14), 4117–4140, doi:10.5194/acp-8-4117-2008, 2008.

Ng, N. L., Brown, S. S., Archibald, A. T., Atlas, E., Cohen, R. C., Crowley, J. N., Day, D. A., Donahue, N. M., Fry, J. L., Fuchs, H., Griffin, R. J., Guzman, M. I., Herrmann, H., Hodzic, A., Iinuma, Y., Jimenez, J. L., Kiendler-Scharr, A., Lee, B. H., Luecken, D. J., Mao, J., McLaren, R., Mutzel, A., Osthoff, H. D., Ouyang, B., Picquet-Varrault, B., Platt, U., Pye, H. O. T., Rudich, Y., Schwantes, R. H., Shiraiwa, M., Stutz, J., Thornton, J. A., Tilgner, A., Williams, B. J. and Zaveri, R. A.: Nitrate radicals and biogenic volatile organic compounds: oxidation, mechanisms, and organic aerosol, Atmos. Chem. Phys., 17(3), 2103–2162, doi:10.5194/acp-17-2103-2017, 2017.

Nguyen, Q. T., Christensen, M. K., Cozzi, F., Zare, A., Hansen, A. M. K., Kristensen, K., Tulinius, T. E., Madsen, H. H., Christensen, J. H., Brandt, J., Massling, A., Nøjgaard, J. K. and Glasius, M.: Understanding the anthropogenic influence on formation of biogenic secondary organic aerosols in Denmark via analysis of organosulfates and related oxidation products, Atmos. Chem. Phys., 14(17), 8961–8981, doi:10.5194/acp-14-8961-2014, 2014.

Nguyen, T. B., Bateman, A. P., Bones, D. L., Nizkorodov, S. A., Laskin, J. and Laskin, A.: High-resolution mass spectrometry analysis of secondary organic aerosol generated by ozonolysis of isoprene, Atmos. Environ., 44(8), 1032–1042, doi:10.1016/J.ATMOSENV.2009.12.019, 2010.

Nguyen, T. B., Bates, K. H., Crounse, J. D., Schwantes, R. H., Zhang, X., Kjaergaard, H. G., Surratt, J. D., Lin, P., Laskin, A., Seinfeld, J. H. and Wennberg, P. O.: Mechanism of the hydroxyl radical oxidation of methacryloyl peroxynitrate (MPAN) and its pathway toward secondary organic aerosol formation in the atmosphere, Phys. Chem. Chem. Phys., 17(27), 17914–17926, doi:10.1039/c5cp02001h, 2015.

None, S., R, G., SK, S. and TK, M.: Seasonal variation, source apportionment and source attributed health risk of fine carbonaceous aerosols over National Capital Region, India, Chemosphere, 237, doi:10.1016/J.CHEMOSPHERE.2019.124500, 2019.

1102 Panopoulou, A., Liakakou, E., Sauvage, S., Gros, V., Locoge, N., Stavroulas, I., Bonsang, B.,
1103 Gerasopoulos, E. and Mihalopoulos, N.: Yearlong measurements of monoterpenes and isoprene in a
1104 Mediterranean city (Athens): Natural vs anthropogenic origin, Atmos. Environ., 243, 117803,
1105 doi:10.1016/J.ATMOSENV.2020.117803, 2020.

1106 Panopoulou, A., Liakakou, E., Sauvage, S., Gros, V., Locoge, N., Bonsang, B., Salameh, T.,
1107 Gerasopoulos, E. and Mihalopoulos, N.: Variability and sources of non-methane hydrocarbons at a
1108 Mediterranean urban atmosphere: The role of biomass burning and traffic emissions, Sci. Total
1109 Environ., 800, 149389, doi:10.1016/J.SCITOTENV.2021.149389, 2021.

1110 Passananti, M., Kong, L., Shang, J., Dupart, Y., Perrier, S., Chen, J., Donaldson, D. J. and George, C.:
1111 Organosulfate Formation through the Heterogeneous Reaction of Sulfur Dioxide with Unsaturated
1112 Fatty Acids and Long-Chain Alkenes, Angew. Chemie - Int. Ed., 55(35), 10336–10339,
1113 doi:10.1002/anie.201605266, 2016.

1114 Paulot, F., Crounse, J. D., Kjaergaard, H. G., Kurten, A., St. Clair, J. M., Seinfeld, J. H. and Wennberg, P.
1115 O.: Unexpected Epoxide Formation in the Gas-Phase Photooxidation of Isoprene, Science (80-.).,
1116 325(5941), 730–733, doi:10.1126/science.1172910, 2009.

1117 Rattanavaraha, W., Chu, K., Budisulistiorini, S. H., Riva, M., Lin, Y.-H., Edgerton, E. S., Baumann, K.,
1118 Shaw, S. L., Guo, H., King, L., Weber, R. J., Neff, M. E., Stone, E. A., Offenberg, J. H., Zhang, Z., Gold, A.
1119 and Surratt, J. D.: Assessing the impact of anthropogenic pollution on isoprene-derived secondary
1120 organic aerosol formation in PM<sub>2.5</sub> collected from the
1121 Birmingham, Alabama, ground site during the 2013 Southern Oxidant and Aerosol Study, Atmos.
1122 Chem. Phys., 16(8), 4897–4914, doi:10.5194/acp-16-4897-2016, 2016a.

1123 Rattanavaraha, W., Chu, K., Budisulistiorini, S. H., Riva, M., Lin, Y. H., Edgerton, E. S., Baumann, K.,
1124 Shaw, S. L., Guo, H., King, L., Weber, R. J., Neff, M. E., Stone, E. A., Offenberg, J. H., Zhang, Z., Gold, A.
1125 and Surratt, J. D.: Assessing the impact of anthropogenic pollution on isoprene-derived secondary
1126 organic aerosol formation in PM2.5 collected from the Birmingham, Alabama, ground site during the
1127 2013 Southern Oxidant and Aerosol Study, Atmos. Chem. Phys., 16(8), 4897–4914, doi:10.5194/acp-
1128 16-4897-2016, 2016b.

1129 Reyes-Villegas, E., Panda, U., Darbyshire, E., Cash, J. M., Joshi, R., Langford, B., Di Marco, C. F.,
1130 Mullinger, N. J., Alam, M. S., Crilley, L. R., Rooney, D. J., Acton, W. J. F., Drysdale, W., Nemitz, E.,
1131 Flynn, M., Voliotis, A., McFiggans, G., Coe, H., Lee, J., Hewitt, C. N., Heal, M. R., Gunthe, S. S., Mandal,
1132 T. K., Gurjar, B. R., Shivani, Gadi, R., Singh, S., Soni, V. and Allan, J. D.: PM1 composition and source
1133 apportionment at two sites in Delhi, India, across multiple seasons, Atmos. Chem. Phys., 21(15),
1134 11655–11667, doi:10.5194/ACP-21-11655-2021, 2021.

1135 Riva, M., Da Silva Barbosa, T., Lin, Y.-H., Stone, E. A., Gold, A. and Surratt, J. D.: Chemical
1136 characterization of organosulfates in secondary organic aerosol derived from the photooxidation of
1137 alkanes, Atmos. Chem. Phys., 16(17), 11001–11018, doi:10.5194/acp-16-11001-2016, 2016a.

1138 Riva, M., Budisulistiorini, S. H., Zhang, Z. and Gold, A.: Chemical characterization of secondary
1139 organic aerosol constituents from isoprene ozonolysis in the presence of acidic aerosol, Atmos.
1140 Environ., 130, 5–13, doi:10.1016/J.ATMOSENV.2015.06.027, 2016b.

1141 Riva, M., Bell, D. M., Hansen, A. M. K., Drozd, G. T., Zhang, Z., Gold, A., Imre, D., Surratt, J. D., Glasius,
1142 M. and Zelenyuk, A.: Effect of Organic Coatings, Humidity and Aerosol Acidity on Multiphase
1143 Chemistry of Isoprene Epoxydiols, Environ. Sci. Technol., 50(11), 5580–5588,
1144 doi:10.1021/acs.est.5b06050, 2016c.

1145 Riva, M., Chen, Y., Zhang, Y., Lei, Z., Olson, N. E., Boyer, H. C., Narayan, S., Yee, L. D., Green, H. S., Cui,
1146 T., Zhang, Z., Baumann, K., Fort, M., Edgerton, E., Budisulistiorini, S. H., Rose, C. A., Ribeiro, I. O., e
1147 Oliveira, R. L., dos Santos, E. O., Machado, C. M. D., Szopa, S., Zhao, Y., Alves, E. G., de Sá, S. S., Hu,

W., Knipping, E. M., Shaw, S. L., Duvoisin Junior, S., de Souza, R. A. F., Palm, B. B., Jimenez, J.-L., Glasius, M., Goldstein, A. H., Pye, H. O. T., Gold, A., Turpin, B. J., Vizuete, W., Martin, S. T., Thornton, J. A., Dutcher, C. S., Ault, A. P. and Surratt, J. D.: Increasing Isoprene Epoxydiol-to-Inorganic Sulfate Aerosol Ratio Results in Extensive Conversion of Inorganic Sulfate to Organosulfur Forms: Implications for Aerosol Physicochemical Properties, Environ. Sci. Technol., acs.est.9b01019, doi:10.1021/acs.est.9b01019, 2019.

Saha, D., Soni, K., Mohanan, M. N. and Singh, M.: Long-term trend of ventilation coefficient over Delhi and its potential impacts on air quality, Remote Sens. Appl. Soc. Environ., 15, 100234, doi:10.1016/J.RSASE.2019.05.003, 2019.

Sahu, L. K. and Saxena, P.: High time and mass resolved PTR-TOF-MS measurements of VOCs at an urban site of India during winter: Role of anthropogenic, biomass burning, biogenic and photochemical sources, Atmos. Res., 164–165, 84–94, doi:10.1016/J.ATMOSRES.2015.04.021, 2015.

Sahu, L. K., Tripathi, N. and Yadav, R.: Contribution of biogenic and photochemical sources to ambient VOCs during winter to summer transition at a semi-arid urban site in India, Environ. Pollut., 229, 595–606, doi:10.1016/J.ENVPOL.2017.06.091, 2017.

Sawlani, R., Agnihotri, R., Sharma, C., Patra, P. K., Dimri, A. P., Ram, K. and Verma, R. L.: The severe Delhi SMOG of 2016: A case of delayed crop residue burning, coincident firecracker emissions, and atypical meteorology, Atmos. Pollut. Res., 10(3), 868–879, doi:10.1016/j.apr.2018.12.015, 2019.

Schindelka, J., Iinuma, Y., Hoffmann, D. and Herrmann, H.: Sulfate radical-initiated formation of isoprene-derived organosulfates in atmospheric aerosols, Faraday Discuss., 165(0), 237–259, doi:10.1039/c3fd00042g, 2013.

Schnell, J. L., Naik, V., Horowitz, L. W., Paulot, F., Mao, J., Ginoux, P., Zhao, M. and Ram, K.: Exploring the relationship between surface PM $_{2.5}$ and meteorology in Northern India, Atmos. Chem. Phys., 18(14), 10157–10175, doi:10.5194/acp-18-10157-2018, 2018.

Sharma, S. K. and Mandal, T. K.: Chemical composition of fine mode particulate matter (PM2.5) in an urban area of Delhi, India and its source apportionment, Urban Clim., 21, 106–122, doi:10.1016/j.uclim.2017.05.009, 2017.

Sheesley, R. J., Kirillova, E., Andersson, A., Krusa, M., Praveen, P. S., Budhavant, K., Safai, P. D., Rao, P. S. P. and Gustafsson, O.: Year-round radiocarbon-based source apportionment of carbonaceous aerosols at two background sites in South Asia, J. Geophys. Res. Atmos., 117(10), doi:10.1029/2011JD017161, 2012.

Simon, M., Dada, L., Heinritzi, M., Scholz, W., Stolzenburg, D., Fischer, L., Wagner, A., Kürten, A., Rörup, B., He, X.-C., Almeida, J., Baalbaki, R., Baccarini, A., Bauer, P., Beck, L., Bergen, A., Bianchi, F., Bräkling, S., Brilke, S., Caudillo, L., Chen, D., Chu, B., Dias, A., Draper, D., Duplissy, J., El Haddad, I., Finkenzeller, H., Frege, C., Gonzalez-Carracedo, L., Gordon, H., Granzin, M., Hakala, J., Hofbauer, V., Hoyle, C., Kim, C., Kong, W., Lamkaddam, H., Lee, C., Lehtipalo, K., Leiminger, M., Mai, H., Manninen, H., Marie, G., Marten, R., Mentler, B., Molteni, U., Nichman, L., Nie, W., Ojdanic, A., Onnela, A., Partoll, E., Petäjä, T., Pfeifer, J., Philippov, M., Quéléver, L., Ranjithkumar, A., Rissanen, M., Schallhart, S., Schobesberger, S., Schuchmann, S., Shen, J., Sipilä, M., Steiner, G., Stozhkov, Y., Tauber, C., Tham, Y., Tomé, A., Vazquez-Pufleau, M., Vogel, A., Wagner, R., Wang, M., Wang, D., Wang, Y., Weber, S., Wu, Y., Xiao, M., Yan, C., Ye, P., Ye, Q., Zauner-Wieczorek, M., Zhou, X., Baltensperger, U., Dommen, J., Flagan, R., Hansel, A., Kulmala, M., Volkamer, R., Winkler, P., Worsnop, D., Donahue, N., Kirkby, J. and Curtius, J.: Molecular understanding of new-particle formation from alpha-pinene between −50 °C and 25 °C, Atmos. Chem. Phys., (January), 1–42, doi:10.5194/acp-2019-1058, 2020.

1194   Sindelarova, K., Granier, C., Bouarar, I., Guenther, A., Tilmes, S., Stavrakou, T., Müller, J. F., Kuhn, U.,
1195   Stefani, P. and Knorr, W.: Global data set of biogenic VOC emissions calculated by the MEGAN model
1196   over the last 30 years, Atmos. Chem. Phys., 14(17), 9317–9341, doi:10.5194/ACP-14-9317-2014,
1197   2014.

1198   Singh, B. P., Kumar, K. and Jain, V. K.: Source identification and health risk assessment associated
1199   with particulate- and gaseous-phase PAHs at residential sites in Delhi, India, Air Qual. Atmos. Heal.,
1200   doi:10.1007/S11869-021-01035-5, 2021.

1201   Singh, D. P., Gadi, R. and Mandal, T. K.: Characterization of Gaseous and Particulate Polycyclic
1202   Aromatic Hydrocarbons in Ambient Air of Delhi, India, Polycycl. Aromat. Compd., 32(4), 556–579,
1203   doi:10.1080/10406638.2012.683230, 2012.

1204   Sinha, V., Kumar, V. and Sarkar, C.: Chemical composition of pre-monsoon air in the Indo-Gangetic
1205   Plain measured using a new air quality facility and PTR-MS: High surface ozone and strong influence
1206   of biomass burning, Atmos. Chem. Phys., 14(12), 5921–5941, doi:10.5194/acp-14-5921-2014, 2014.

1207   Spolnik, G., Wach, P., Rudzinski, K. J., Skotak, K., Danikiewicz, W. and Szmigielski, R.: Improved
1208   UHPLC-MS/MS Methods for Analysis of Isoprene-Derived Organosulfates, Anal. Chem., 90(5), 3416–
1209   3423, doi:10.1021/acs.analchem.7b05060, 2018.

1210   Stewart, G. J., Nelson, B. S., Acton, W. J. F., Vaughan, A. R., Farren, N. J., Hopkins, J. R., Ward, M. W.,
1211   Swift, S. J., Arya, R., Mondal, A., Jangirh, R., Ahlawat, S., Yadav, L., Sharma, S. K., Yunus, S. S. M.,
1212   Hewitt, C. N., Nemitz, E., Mullinger, N., Gadi, R., Sahu, L. K., Tripathi, N., Rickard, A. R., Lee, J. D.,
1213   Mandal, T. K. and Hamilton, J. F.: Emissions of intermediate-volatility and semi-volatile organic
1214   compounds from domestic fuels used in Delhi, India, Atmos. Chem. Phys., 21(4), 2407–2426,
1215   doi:10.5194/ACP-21-2407-2021, 2021a.

1216   Stewart, G. J., Acton, W. J. F., Nelson, B. S., Vaughan, A. R., Hopkins, J. R., Arya, R., Mondal, A.,
1217   Jangirh, R., Ahlawat, S., Yadav, L., Sharma, S. K., Dunmore, R. E., Yunus, S. S. M., Nicholas Hewitt, C.,
1218   Nemitz, E., Mullinger, N., Gadi, R., Sahu, L. K., Tripathi, N., Rickard, A. R., Lee, J. D., Mandal, T. K. and
1219   Hamilton, J. F.: Emissions of non-methane volatile organic compounds from combustion of domestic
1220   fuels in Delhi, India, Atmos. Chem. Phys., 21(4), 2383–2406, doi:10.5194/ACP-21-2383-2021, 2021b.

1221   Stewart, G. J., Nelson, B. S., Drysdale, W. S., Acton, W. J. F., Vaughan, A. R., Hopkins, J. R., Dunmore,
1222   R. E., Hewitt, C. N., Nemitz, E., Mullinger, N., Langford, B., Shivani, Reyes-Villegas, E., Gadi, R.,
1223   Rickard, A. R., Lee, J. D. and Hamilton, J. F.: Sources of non-methane hydrocarbons in surface air in
1224   Delhi, India, Faraday Discuss., 226(0), 409–431, doi:10.1039/D0FD00087F, 2021c.

1225   Surratt, J. D., Murphy, S. M., Kroll, J. H., Ng, N. L., Hildebrandt, L., Sorooshian, A., Szmigielski, R.,
1226   Vermeylen, R., Maenhaut, W., Claeys, M., Flagan, R. C. and Seinfeld, J. H.: Chemical composition of
1227   secondary organic aerosol formed from the photooxidation of isoprene, J. Phys. Chem. A, 110(31),
1228   9665–9690, doi:10.1021/jp061734m, 2006.

1229   Surratt, J. D., Kroll, J. H., Kleindienst, T. E., Edney, E. O., Claeys, M., Sorooshian, A., Ng, N. L.,
1230   Offenberg, J. H., Lewandowski, M., Jaoui, M., Flagan, R. C. and Seinfeld, J. H.: Evidence for
1231   Organosulfates in Secondary Organic Aerosol, Environ. Sci. Technol., 41(2), 517–527,
1232   doi:10.1021/es062081q, 2007.

1233   Surratt, J. D., Gómez-González, Y., Chan, A. W. H., Vermeylen, R., Shahgholi, M., Kleindienst, T. E.,
1234   Edney, E. O., Offenberg, J. H., Lewandowski, M., Jaoui, M., Maenhaut, W., Claeys, M., Flagan, R. C.
1235   and Seinfeld, J. H.: Organosulfate Formation in Biogenic Secondary Organic Aerosol, J. Phys. Chem. A,
1236   112(36), 8345–8378, doi:10.1021/jp802310p, 2008a.

1237   Surratt, J. D., Gómez-González, Y., Chan, A. W. H., Vermeylen, R., Shahgholi, M., Kleindienst, T. E.,
1238   Edney, E. O., Offenberg, J. H., Lewandowski, M., Jaoui, M., Maenhaut, W., Claeys, M., Flagan, R. C.

and Seinfeld, J. H.: Organosulfate Formation in Biogenic Secondary Organic Aerosol, J. Phys. Chem. A, 112(36), 8345–8378, doi:10.1021/jp802310p, 2008b.

Surratt, J. D., Chan, A. W. H., Eddingsaas, N. C., Chan, M., Loza, C. L., Kwan, A. J., Hersey, S. P., Flagan, R. C., Wennberg, P. O. and Seinfeld, J. H.: Reactive intermediates revealed in secondary organic aerosol formation from isoprene, Proc. Natl. Acad. Sci., 107(15), 6640–6645, doi:10.1073/pnas.0911114107, 2010.

Szidat, S., Jenk, T. M., Gäggeler, H. W., Synal, H. A., Fisseha, R., Baltensperger, U., Kalberer, M., Samburova, V., Wacker, L., Saurer, M., Schwikowski, M. and Hajdas, I.: Source apportionment of aerosols by 14C measurements in different carbonaceous particle fractions, in Radiocarbon, vol. 46, pp. 475–484, University of Arizona., 2004.

Takeuchi, M. and Ng, N. L.: Chemical composition and hydrolysis of organic nitrate aerosol formed from hydroxyl and nitrate radical oxidation of α-pinene and β-pinene, Atmos. Chem. Phys., 19(19), 12749–12766, doi:10.5194/ACP-19-12749-2019, 2019.

Wagner, P. and Kuttler, W.: Biogenic and anthropogenic isoprene in the near-surface urban atmosphere — A case study in Essen, Germany, Sci. Total Environ., 475, 104–115, doi:10.1016/J.SCITOTENV.2013.12.026, 2014.

Wang, J. L., Chew, C., Chang, C. Y., Liao, W. C., Lung, S. C. C., Chen, W. N., Lee, P. J., Lin, P. H. and Chang, C. C.: Biogenic isoprene in subtropical urban settings and implications for air quality, Atmos. Environ., 79, 369–379, doi:10.1016/J.ATMOSENV.2013.06.055, 2013.

Wang, X., Hayeck, N., Brüggemann, M., Yao, L., Chen, H., Zhang, C., Emmelin, C., Chen, J., George, C. and Wang, L.: Chemical Characteristics of Organic Aerosols in Shanghai: A Study by Ultrahigh-Performance Liquid Chromatography Coupled With Orbitrap Mass Spectrometry, J. Geophys. Res. Atmos., 122(21), 11,703-11,722, doi:10.1002/2017JD026930, 2017.

Wang, X. K., Rossignol, S., Ma, Y., Yao, L., Wang, M. Y., Chen, J. M., George, C. and Wang, L.: Molecular characterization of atmospheric particulate organosulfates in three megacities at the middle and lower reaches of the Yangtze River, Atmos. Chem. Phys., 16(4), 2285–2298, doi:10.5194/acp-16-2285-2016, 2016.

Wang, Y., Hu, M., Guo, S., Wang, Y., Zheng, J., Yang, Y., Zhu, W., Tang, R., Li, X., Liu, Y., Le Breton, M., Du, Z., Shang, D., Wu, Y., Wu, Z., Song, Y., Lou, S., Hallquist, M. and Yu, J.: The secondary formation of organosulfates under interactions between biogenic emissions and anthropogenic pollutants in summer in Beijing, Atmos. Chem. Phys., 18(14), 10693–10713, doi:10.5194/acp-18-10693-2018, 2018a.

Wang, Y., Hu, M., Guo, S., Wang, Y., Zheng, J., Yang, Y., Zhu, W., Tang, R., Li, X., Liu, Y., Le Breton, M., Du, Z., Shang, D., Wu, Y., Wu, Z., Song, Y., Lou, S., Hallquist, M. and Yu, J.: The secondary formation of organosulfates under interactions between biogenic emissions and anthropogenic pollutants in summer in Beijing, Atmos. Chem. Phys., 18(14), 10693–10713, doi:10.5194/acp-18-10693-2018, 2018b.

Wang, Y., Tong, R. and Yu, J. Z.: Chemical Synthesis of Multifunctional Air Pollutants: Terpene-Derived Nitrooxy Organosulfates, Environ. Sci. Technol., acs.est.1c00348, doi:10.1021/acs.est.1c00348, 2021a.

Wang, Y., Zhao, Y., Wang, Y., Yu, J. Z., Shao, J., Liu, P., Zhu, W., Cheng, Z., Li, Z., Yan, N. and Xiao, H.: Organosulfates in atmospheric aerosols in shanghai, china: Seasonal and interannual variability, origin, and formation mechanisms, Atmos. Chem. Phys., 21(4), 2959–2980, doi:10.5194/acp-21-2959-2021, 2021b.

Wennberg, P. O., Bates, K. H., Crounse, J. D., Dodson, L. G., McVay, R. C., Mertens, L. A., Nguyen, T. B., Praske, E., Schwantes, R. H., Smarte, M. D., St Clair, J. M., Teng, A. P., Zhang, X. and Seinfeld, J. H.: Gas-Phase Reactions of Isoprene and Its Major Oxidation Products, Chem. Rev., 118(7), 3337–3390, doi:10.1021/acs.chemrev.7b00439, 2018.

WHO: WHO | Ambient air pollution, WHO, 2018.

Wozniak, A. S., Bauer, J. E. and Dickhut, R. M.: Characteristics of water-soluble organic carbon associated with aerosol particles in the eastern United States, Atmos. Environ., 46, 181–188, doi:10.1016/j.atmosenv.2011.10.001, 2012.

Xu, J., Song, S., Harrison, R. M., Song, C., Wei, L., Zhang, Q., Sun, Y., Lei, L., Zhang, C., Yao, X., Chen, D., Li, W., Wu, M., Tian, H., Luo, L., Tong, S., Li, W., Wang, J., Shi, G., Huangfu, Y., Tian, Y., Ge, B., Su, S., Peng, C., Chen, Y., Yang, F., Mihajlidi-Zelić, A., Đorđević, D., Swift, S. J., Andrews, I., Hamilton, J. F., Sun, Y., Kramawijaya, A., Han, J., Saksakulkrai, S., Baldo, C., Hou, S., Zheng, F., Daellenbach, K. R., Yan, C., Liu, Y., Kulmala, M., Fu, P. and Shi, Z.: An interlaboratory comparison of aerosol inorganic ion measurements by ion chromatography: Implications for aerosol pH estimate, Atmos. Meas. Tech., 13(11), 6325–6341, doi:10.5194/AMT-13-6325-2020, 2020.

Xu, L., Guo, H., Boyd, C. M., Klein, M., Bougiatioti, A., Cerully, K. M., Hite, J. R., Isaacman-VanWertz, G., Kreisberg, N. M., Knote, C., Olson, K., Koss, A., Goldstein, A. H., Hering, S. V., Gouw, J. de, Baumann, K., Lee, S.-H., Nenes, A., Weber, R. J. and Ng, N. L.: Effects of anthropogenic emissions on aerosol formation from isoprene and monoterpenes in the southeastern United States, Proc. Natl. Acad. Sci., 112(1), 37–42, doi:10.1073/PNAS.1417609112, 2015.

Yadav, A. K., Sarkar, S., Jyethi, D. S., Rawat, P., Aithani, D., Siddiqui, Z. and Khillare, P. S.: Fine Particulate Matter Bound Polycyclic Aromatic Hydrocarbons and Carbonaceous Species in Delhi's Atmosphere: Seasonal Variation, Sources, and Health Risk Assessment, Aerosol Sci. Eng. 2021 52, 5(2), 193–213, doi:10.1007/S41810-021-00094-6, 2021.

Yee, L. D., Isaacman-VanWertz, G., Wernis, R. A., Kreisberg, N. M., Glasius, M., Riva, M., Surratt, J. D., de Sá, S. S., Martin, S. T., Alexander, M. L., Palm, B. B., Hu, W., Campuzano-Jost, P., Day, D. A., Jimenez, J. L., Liu, Y., Misztal, P. K., Artaxo, P., Viegas, J., Manzi, A., de Souza, R. A. F., Edgerton, E. S., Baumann, K. and Goldstein, A. H.: Natural and Anthropogenically Influenced Isoprene Oxidation in Southeastern United States and Central Amazon, Environ. Sci. Technol., doi:10.1021/acs.est.0c00805, 2020.

Zhang, H., Yee, L. D., Lee, B. H., Curtis, M. P., Worton, D. R., Isaacman-VanWertz, G., Offenberg, J. H., Lewandowski, M., Kleindienst, T. E., Beaver, M. R., Holder, A. L., Lonneman, W. A., Docherty, K. S., Jaoui, M., Pye, H. O. T., Hu, W., Day, D. A., Campuzano-Jost, P., Jimenez, J. L., Guo, H., Weber, R. J., De Gouw, J., Koss, A. R., Edgerton, E. S., Brune, W., Mohr, C., Lopez-Hilfiker, F. D., Lutz, A., Kreisberg, N. M., Spielman, S. R., Hering, S. V., Wilson, K. R., Thornton, J. A. and Goldstein, A. H.: Monoterpenes are the largest source of summertime organic aerosol in the southeastern United States, Proc. Natl. Acad. Sci. U. S. A., 115(9), 2038–2043, doi:10.1073/pnas.1717513115, 2018.

Zhang, H., Zhang, Y., Huang, Z., Acton, W. J. F., Wang, Z., Nemitz, E., Langford, B., Mullinger, N., Davison, B., Shi, Z., Liu, D., Song, W., Yang, W., Zeng, J., Wu, Z., Fu, P., Zhang, Q. and Wang, X.: Vertical profiles of biogenic volatile organic compounds as observed online at a tower in Beijing, J. Environ. Sci., 95, 33–42, doi:10.1016/J.JES.2020.03.032, 2020.

Zhao, D., Schmitt, S. H., Wang, M., Acir, I. H., Tillmann, R., Tan, Z., Novelli, A., Fuchs, H., Pullinen, I., Wegener, R., Rohrer, F., Wildt, J., Kiendler-Scharr, A., Wahner, A. and Mentel, T. F.: Effects of NOx and SO2 on the secondary organic aerosol formation from photooxidation of α-pinene and limonene, Atmos. Chem. Phys., 18(3), 1611–1628, doi:10.5194/acp-18-1611-2018, 2018.

Zhao, D. F., Kaminski, M., Schlag, P., Fuchs, H., Acir, I. H., Bohn, B., Häseler, R., Kiendler-Scharr, A.,

1329   Rohrer, F., Tillmann, R., Wang, M. J., Wegener, R., Wildt, J., Wahner, A. and Mentel, T. F.: Secondary
1330   organic aerosol formation from hydroxyl radical oxidation and ozonolysis of monoterpenes, Atmos.
1331   Chem. Phys., 15(2), 991–1012, doi:10.5194/ACP-15-991-2015, 2015.

1332   Zou, Y., Deng, X. J., Deng, T., Yin, C. Q. and Li, F.: One-year characterization and reactivity of isoprene
1333   and its impact on surface ozone formation at a suburban site in Guangzhou, China, Atmosphere
1334   (Basel)., 10(4), doi:10.3390/ATMOS10040201, 2019.

1335